

**DEMOCRATIC AND POPULAR REPUBLIC OF ALGERIA**  
**MINISTRY OF HIGH EDUCATION AND SCIENTIFIC RESEARCH**  
**UNIVERSITY OF MOHAMED BOUDIAF - M'SILA**

**FACULTY OF SCIENCES**  
**DEPARTMENT OF PHYSICS**

**N° : PH/ENR/08/2024**



**DOMAINE: SCIENCE OF MATTER**  
**FIELD : PHYSICS**  
**OPTION : PHYSICS OF ENERGY**  
**AND RENEWABLE ENERGIES**

**Thesis Submitted for Obtaining**  
**Diploma of Academic Master**

**By:**

**Ben mehenni Rouaa**

**Entitled**

**Pressure and temperature influences on thermal and  
thermoelectric properties of some materials used in  
thermoelectric generators**

**Defended on 10/06/2024 in front of a jury composed of:**

<b>Mohammed Elamin Ketfi</b>	<b>University of Msila</b>	<b>Chairman</b>
<b>Saber Saad Essaoud</b>	<b>University of Msila</b>	<b>Supervisor</b>
<b>RAGHDI Amina</b>	<b>University of Msila</b>	<b>Examiner</b>

**Academic Year: 2023/2024**

# شكر و عرفان

أول من يشكر و يحمد آناء الليل و أطراف النهار هو العلي القهار الأول و الآخر في الظاهر و الباطن، الذي أغرقنا بنعمه التي لا تحصى، و أغدق علينا برزقه الذي لا يفنى، و أنار دروبنا فله جزيل الحمد و الثناء العظيم، هو الذي أنعم علينا إذ أرسل فينا عبده و رسوله محمد بن عبد الله عليه أسمى الصلوات و أظهر التسليم، أرسله بقرآنه المبين، فعلمنا ما لم يعلم، وحثنا على طلب العلم أينما وجد

لله الحمد كله و الشكر كله أن وفقنا و ألهمنا الصبر على المشاق التي واجهتنا. و الشكر موصول إلى كل معلم أفادنا بعلمه، من أولى المراحل الدراسية حتى هذه اللحظة

كما نرفع كلمة شكر إلى الدكتور المشرف صابر سعد السعود، على كل ما قدمه لنا من توجيهات و معلومات قيمة ساهمت في إثراء موضوع دراستنا.

ونتقدم بجزيل الشكر إلى الأستاذ كتفي محمد الأمين على تفضله برئاسة لجنة المناقشة

و الأستاذة رغدي أمينة على قبولها تقييم هذا العمل المتواضع

وفي الأخير لا يسعنا إلا أن ندعو الله عز وجل أن يرزقنا السداد و الرشاد و العفاف و الغنى و الهداية.

رؤى

# إهداء إلى غزة

إلى غزة، إلى أرض الفخر والعزة إلى منبع الكبرياء والكرامة،  
إلى أرض الأحرار التي لم تتحن للعواصف ولا انكسرت أمام الأهوال.  
إلى كل شبر من ترابك الطاهر  
إلى كل مقاوم يحمي شرف الأمة  
إلى كل أم تحتضن أطفالها بين أهوال القصف  
إلى كل شاب وشابة يبنون بعرقهم حلم الوطن الحر  
إلى كل طفل يرسم في خياله عالماً أجمل رغم الدمار  
إلى كل صحفي وقف في وجه الظلم والظلام بالكلمة والصورة  
إلى غزة، إلى حكاية لم تنته، وقصيدة لم تكتمل، يا نبضاً في قلوب الأحرار  
نحن معكم بقلوبنا وعقولنا، ونحلم بيوم تشرق فيه شمس السلام  
نسأل الله أن ينصركم ويحفظكم، وأن يكتب لكم فجرًا جديدًا يحمل في طياته الأمان والحرية.

رؤى

## TABLE OF CENTENTS

Table of centents	
List of figures	
List of tables	
General introduction	1
<b>CHAPTER 1: THEORETICAL STUDY OF MANY-PARTICLES SYSTEM</b>	
1- The Schrödinger Equation	4
2- Born-Oppenheimer Approximation	5
3- Hartree and Hartree-Fock Approximations (HF)	6
4- Density Functional Theory (DFT)	8
4-1 Formalism of Density Functional Theory (DFT)	10
I. The Theorems of Hohenburg and Kohn	10
II. The Kohn - Sham equation	11
1- Solution of the Kohn - Sham Equation	13
5-The Different Types of Approximation of the	16
5-1 Local density approximation (LSDA)	16
5-2 The Generalized Gradient Approximation GGA	16
6- Full-Potential Linearized Augmented Plane-wave Method (FP-LAPW)	17
6-1 The Plane Wave method (APW)	17
6-2 The Linearized Augmented Plane Wave Method (LAPW)	18
7-Simulation Code WIEN2K	20
<b>CHAPTER 2: RESULTS AND DISCUSSION</b>	
1) Introduction	27
2) Calculation Details	27
3) Results and discussions	28
3-1) Structural properties	28
3-2) Electronic Properties	33
3-2-1) Energy Bands	33
4- The Thermodynamic Properties	38
4-1 Heat Capacities	38
4-2 Entropy	40
4-3 Thermal Expansion Coefficient	42
5- thermoelectric Properties	44
5-1 Seebeck Coefficient	44
5-2 Electrical Conductivity	46
5-3 Electronic Thermal Conductivity:	47
5-4 ZT Factor	49
6) References	51
General conclusion	53

## List of Figures

<b>CHAPTER 1 : DENSITY FUNCTIONAL THEORY- AN OVERVIEW</b>	
<b>Figure I. 1:</b> Self-consistent calculation flowchart	15
<b>Figure I. 2:</b> Diagram of the distribution of the elementary cell in atomic spheres and in interstitial region	17
<b>Figure I. 3:</b> The flowchart of the Wien2k code subroutines	23
<b>Chapter 2:</b>	
<b>Figure II.1:</b> Crystal structure of $\text{CaSnO}_3$ and $\text{MgSnO}_3$	29
<b>Figure II.2:</b> Total Energy-Volume and volume-pressure Curves of $\text{MgSnO}_3$ calculated using GGA-sol approximations.	31
<b>Figure II.3:</b> Total Energy-Volume and volume-pressure Curves of $\text{CaSnO}_3$ calculated using GGA-sol approximations.	33
<b>Figure II.4:</b> band structure spectra for both compounds $\text{MgSnO}_3$ and $\text{CaSnO}_3$	34
<b>Figure II.5:</b> Total and partial density of states of $\text{MgSnO}_3$	36
<b>Figure II.6:</b> Total and partial density of states of $\text{CaSnO}_3$	37
<b>Figure II.7:</b> Variation in the heat capacity "Cv" of the compound $\text{MgSnO}_3$ as a function of temperature	39
<b>Figure II.8:</b> Variation in the heat capacity "Cv" of the compound $\text{CaSnO}_3$ as a function of temperature	39
<b>Figure II.9:</b> Variation in the entropy (S) vary with changes in temperature of $\text{CaSnO}_3$	41
<b>Figure II.10:</b> Variation in the entropy (S) vary with changes in temperature of $\text{MgSnO}_3$	41
<b>Figure II.11:</b> Variation in the thermal expansion coefficient ( $\alpha$ ) vary with changes and temperature of $\text{CaSnO}_3$	43
<b>Figure II.12:</b> Variation in the thermal expansion coefficient ( $\alpha$ ) vary with changes in temperature of $\text{MgSnO}_3$	43
<b>Figure II.13:</b> Variation in the Seebeck coefficient at different temperatures vary with changes in chemical potential of $\text{CaSnO}_3$	45
<b>Figure II.14:</b> Variation in the Seebeck coefficient at different temperatures vary with changes in chemical potential of $\text{MgSnO}_3$	45

<b>Figure II.15:</b> The electrical conductivity at different temperatures varies with changes in the chemical potential for $\text{CaSnO}_3$ compound	46
<b>Figure II.16:</b> The electrical conductivity at different temperatures varies with changes in chemical potential of $\text{MgSnO}_3$	47
<b>Figure II.17:</b> The electronic thermal conductivity at different temperatures varies with changes in chemical potential of $\text{CaSnO}_3$	48
<b>Figure II.18:</b> The electronic thermal conductivity at different temperatures varies with changes in chemical potential of $\text{MgSnO}_3$	48
<b>Figure II.19:</b> The electrical conductivity at different temperatures varies with changes in chemical potential of $\text{CaSnO}_3$	50
<b>Figure II.20:</b> The electrical conductivity at different temperatures varies with changes in chemical potential of $\text{MgSnO}_3$	50

## List of Tables

<b>CHAPTER1 : DENSITY FUNCTIONAL THEORY- AN OVERVIEW</b>	
<b>Table I-1:</b> Comparison between the two methods, Hartree-Fock and the Density Functional Theory	09
<b>CHAPTER2 :</b>	
<b>Table II-1:</b> Values of the structural parameters obtained for <b>MgSnO<sub>3</sub></b> and <b>CaSnO<sub>3</sub></b> compounds and calculated by GGA approximation	30

# INTRODUCTION

---

### Introduction :

---

Solid-state physics plays a crucial role in comprehending natural materials and innovating new ones, vital for diverse applications. Material exploration involves experimental, semi-experimental, and theoretical methods, with the latter gaining prominence due to advanced simulations [1]. Tailored software enables precise analysis, overcoming limitations like time and expense. Continuous software updates refine solution techniques, highlighting the necessity of understanding electronic structures for accurate property interpretation. Various methods stemming from Density Functional Theory (DFT) assist in solving the Schrödinger equation, unveiling insights into structural, elastic, and mechanical characteristics [2]. Perovskite structures, known for their stability and versatile applications, have long captivated scientific interest [3]. The term "perovskite" originated from  $\text{CaTiO}_3$ , discovered in 1839, named after Russian mineralogist Lev Aleksevich von Perovski [4].

The aim of this study is to enhance our comprehension of the structural, electronic, thermodynamic, and thermoelectric properties of perovskite compounds  $\text{MgSnO}_3$  and  $\text{CaSnO}_3$  using the Wien2k calculation software. This research is divided into two primary chapters. The first chapter offers a theoretical foundation for analyzing crystalline systems, drawing upon principles of quantum mechanics. It begins with an exploration of the time-independent Schrödinger equation, which describes the behavior of electrons and nuclei within a system. Significant approximations such as the Born-Oppenheimer, Hartree, Hartree-Fock, and Density Functional Theory (DFT) are explained, focusing particularly on their role in estimating exchange-correlation interactions among electrons..

In the second chapter, we applied theoretical concepts from the first chapter using the Wien2k program [5]. Structural properties like lattice constants, bulk modulus, and cohesive energy were calculated using the Generalized Gradient Approximation (GGA) for exchange-correlation functional [6]. Electronic properties, such as bandgap values and contributing electronic orbitals, were investigated. Then, using the GIBBS2 program [7,8] based on the quasi-harmonic Debye model [9], we explored the effects of temperature and doping on thermodynamic properties like heat capacity, thermal expansion coefficient, and entropy. Finally, employing the BOLTZTRAP2 program, we analyzed various electrical and thermal properties including the Seebeck coefficient, electronic conductivity, and electronic thermal conductivity [10]. A comprehensive summary of the obtained results was provided.

## References

- [1] P. Amaud, (chimie physique) édition dunod (2001).
- [2] E. Schrödinger, Ann. Phys. 79. 361 (1926)
- [3] Hossain, A., Roy, S., & Sakthipandi, K. (2019). The external and internal influences on the tuning of the properties of perovskites: an overview. *Ceramics International*, 45(4), 4152-4166
- [4] Souza, E. C. C. D., & Muccillo, R. (2010). Properties and applications of perovskite proton conductors. *Materials Research*, 13(3), 385-394
- [5] P. Blaha, K. Schwarz, G. Madsen, D. Kvasnicka, J. Luitz, Wien2k, (2001).
- [6] J.P. Perdew, K. Burke, M. Ernzerhof, Generalized Gradient Approximation Made Simple, *Phys. Rev. Lett.* 77 (1996) 3865–3868. <https://doi.org/10.1103/physrevlett.77.3865>.
- [7] V.L. A. Otero-de-la-Roza, D. Abbasi-Pérez, Gibbs2: A new version of the quasiharmonic model code. II. Models for solid-state thermodynamics, features and implementation, *Comput. Phys. Commun.* 182(10) (2011) 2232–2248.
- [8] V.L. A. Otero-de-la-Roza, Gibbs2: A new version of the quasi-harmonic model code. I. Robust treatment of the static data, *Comput. Phys. Commun.* 182(8)(2011) 1708–1720.
- [9] P. Debye, Einige Bemerkungen zur Magnetisierung bei tiefer Temperatur, *Ann. Phys.* 386 (1926) 1154–1160. <https://doi.org/10.1002/andp.19263862517>.
- [10] G.K. Madsen, D.J. Singh, BoltzTraP. A code for calculating band-structure dependent quantities, *Comput. Phys. Commun.* 175 (2006) 67–71.

## **CHAPTER 1:**

# **THEORETICAL STUDY OF MANY-PARTICLES SYSTEM**

---

## CHAPTER 1:

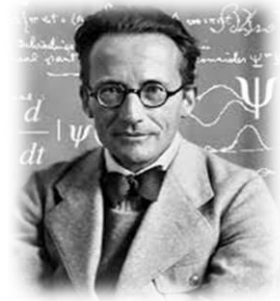
## THEORETICAL STUDY OF MANY-PARTICLES SYSTEM

**Table of Contents**

Table of Contents .....	3
1- The Schrödinger Equation .....	4
2- Born-Oppenheimer Approximation.....	5
3- Hartree and Hartree-Fock Approximations (HF).....	6
4- Density Functional Theory (DFT).....	8
4-1 Formalism of Density Functional Theory (DFT) .....	10
I. Hohenburg and Kohn Theorems.....	10
II. The Kohn - Sham equation.....	11
1- Solution of the Kohn - Sham Equation.....	13
5-The Different Types of Approximation of the <i>Excp</i> .....	16
5-1 Local density approximation (LSDA) .....	16
5-2 The Generalized Gradient Approximation GGA.....	16
6- Full-Potential Linearized Augmented Plane-wave Method FP-LAPW.....	17
6-1 The Plane Wave method (APW) .....	17
6-2 The Linearized Augmented Plane Wave Method (FP-LAPW) .....	18
7- WIEN2K software .....	20
8- References .....	23

## 1- The Schrödinger Equation

Schrödinger, an Austrian theoretical physicist, made significant contributions to the wave theory of matter and was influenced by the concepts of the early quantum theory as developed by Max Planck, Albert Einstein, Niels Bohr, and others.



In 1926, Schrödinger proposed a partial differential equation known as the Schrödinger equation in the framework of quantum theory [1]. The solution of this equation accurately calculated the energy levels of electrons in atoms and describe the instantaneous quantum state of a system through its wave function, which includes all the information about the system studied [2–4]. The Schrödinger equation has the following expression :

$$H\Psi(\vec{R}_I, \vec{r}_i) = E\Psi(\vec{R}_I, \vec{r}_i) \quad (I.1)$$

The two vectors  $\vec{R}_I$  and  $\vec{r}_i$  are the coordinates of the nucleus (I) and of the electron (i).

H: Hamiltonian operator related to the sum of the kinetic energy and the potential energy of the system.

E: eigenvalue Energy of the system.

$\Psi$ : wave function which depends on the coordinates of electrons and nuclei.

The Hamiltonian system - made up of nuclei and electrons - includes the kinetic energy of electrons and nuclei, as well as the potential energies (electron-electron, electron-nucleus, and nucleus-nucleus), therefore the expression of the total Hamiltonian of the system is written by the following expression:

$$H = T_e + T_N + V_{ee} + V_{e-N} + V_{N-N} \quad (I.2)$$

$$T_e = -\sum_i \frac{\hbar^2}{2m_i} \vec{\nabla}_i^2 \rightarrow \text{Electronic kinetic energy (} m_i \text{ the mass of electron } i \text{)}.$$

$$T_n = -\sum_I \frac{\hbar^2}{2m_I} \vec{\nabla}_I^2 \rightarrow \text{Nuclei kinetic energy (} m_I \text{ the mass of the nucleus } I \text{)}.$$

$V_{N-N} = \sum_{I \neq J} \frac{Z_I Z_J e^2}{|R_I - R_J|} \rightarrow$  The interaction part between the nuclei.

$V_{e-N} = \sum_{I,j} \frac{Z_I e^2}{|R_I - r_j|} \rightarrow$  The nuclei-electrons interaction part.

$V_{e-e} = \sum_{i \neq j} \frac{e^2}{|r_i - r_j|} \rightarrow$  The interaction part between the electrons.

$|R_\alpha - R_\beta| \rightarrow$  The distance between the two nuclei  $\alpha$  and  $\beta$

$|r_i - R_\alpha| \rightarrow$  The distance between the nucleus  $\alpha$  and the electron  $i$

$|r_i - r_j| \rightarrow$  The distance between the two electrons  $i$  and  $j$ .

solving the Schrödinger equation can be really hard, especially for systems with lots of electrons and moving parts, and their complicated interactions. Because it's so complicated, we usually can't find exact answers. So, scientists use simpler methods and guesses to get close to the right answer. Here are some of the main ways they do that:

## 2- Born-Oppenheimer Approximation



The Born-Oppenheimer approximation [5], developed in 1927 by physicists Max Born and Robert Oppenheimer, it is one of the basic concepts underlying the description of the quantum states of molecules. This approximation makes it possible to separate the motion of the nuclei and the motion of the electrons. Despite its movement, the nucleus remains very close to its equilibrium position with respect to the electrons, which are very fast, and thus



it is possible to ignore the nuclei's kinetic energy in regards to the electrons' kinetic energy and consider the nucleus-nucleus interaction energy as a constant quantity ( $V_{nn} = \text{Constant}$ ).

According to the Born-Oppenheimer approximation we can rewrite the total wave function of the system  $\Psi(\vec{R}_I^0, \vec{r}_i)$  in the form of a product of an electronic function  $\Psi_e(\vec{R}_I^0, \vec{r}_i)$  and a nuclear

function  $\Psi_n(\vec{R}_I^0)$ , thus, we can separate the motion of nuclei from that of electrons. Then the wave function is written:

$$\Psi(\vec{R}_I^0, \vec{r}_i) = \Psi_n(\vec{R}_I^0) \Psi_e(\vec{R}_I^0, \vec{r}_i) \quad (I.3)$$

$$\begin{cases} [T_e + V_{ee} + V_{en}] \Psi_e(\vec{R}_I^0, \vec{r}_i) = E_e(\vec{R}_I^0) \Psi_e(\vec{R}_I^0, \vec{r}_i) \\ [T_n + V_{nn} + E_e(\vec{R}_I^0)] \Psi_n(\vec{R}_I^0) = E \Psi_n(\vec{R}_I^0) \end{cases} \quad (I.4)$$

Despite employing this simplification to the Schrödinger equation, the problem persists as challenging to solve, primarily due to the intricate nature of electron-electron interactions. Current mathematical methods are insufficient for resolving the complexities involved, prompting the need for further approximations.

### 3- Hartree and Hartree-Fock Approximations (HF)

The Hartree-Fock approximation was introduced to address and rectify the shortcomings of the Hartree approximation, which was initially proposed by Hartree in 1928[6,7]. That all electrons be treated as identical particles that move independently without interacting with other particles (independent particle approximation[8]). In this approximation, Hartree treats the interactions between electrons as particles carrying a charge without taking into account the spin state. The interactions are simplified to Coulombic repulsion interactions, overlooking both exchange and correlation terms. Additionally, the wave function lacks "anti-symmetry" as it does not account for the Pauli exclusion principle.[3,4].



Although the Hartree approximation overlooks electron spin and the Pauli exclusion principle, it simplifies the Schrödinger equation by reducing the study of a large number of electrons to that of a single electron., so that the total Hamiltonian H of electrons is the sum of the Hamiltonians  $h_i$  of each electron, while the total wave function of the electronic system represents by multiplication the individual wave functions of each electron [3,4].

Finally, the total energy of the electronic system is the aggregate of the energies of all electrons. Following Hartree's approximation, the Hamiltonian equation for a single electron can be expressed as follows:

$$H = \sum_i h_i \quad (\text{I.5})$$

$$h_i = -\frac{\hbar^2}{2m_i} \Delta_i - \sum_l \frac{Z_l e^2}{|\vec{r}_i - \vec{R}_l|} + \frac{1}{2} \sum_j \frac{e^2}{|\vec{r}_i - \vec{r}_j|} \quad (\text{I.6})$$

$$\Psi_e = \prod_i \Psi_i \quad (\text{I.7})$$

$$E_e = \sum_i \varepsilon_i \quad (\text{I.8})$$

In 1930, Fock [9] improved and refined Hartree's model by replacing electron wave functions with a Slater determinant[10]. This change allowed Fock to address the exchange effect, which Hartree had overlooked. As a result, the interaction between electrons now includes both Coulomb interaction and the exchange effect. This led to the replacement of previous functions with anti-symmetric functions. In his analysis of electronic interactions, Fock introduced the concept of "spin" and replaced the electronic system's wave function with a Slater determinant, as expressed by the formula:



$$\Psi_{HF}(\vec{r}_1, \vec{r}_2, \vec{r}_3, \dots, \vec{r}_N) = \frac{1}{\sqrt{N_e!}} \begin{bmatrix} \Psi_1(\vec{r}_1) & \Psi_1(\vec{r}_2) & \Psi_1(\vec{r}_3) & \cdots & \Psi_1(\vec{r}_N) \\ \Psi_2(\vec{r}_1) & \Psi_2(\vec{r}_2) & \Psi_2(\vec{r}_3) & \cdots & \Psi_2(\vec{r}_N) \\ \Psi_3(\vec{r}_1) & \Psi_3(\vec{r}_2) & \Psi_3(\vec{r}_3) & \cdots & \Psi_3(\vec{r}_N) \\ \vdots & \vdots & \vdots & \ddots & \vdots \\ \Psi_N(\vec{r}_1) & \Psi_N(\vec{r}_2) & \Psi_N(\vec{r}_3) & \cdots & \Psi_N(\vec{r}_N) \end{bmatrix} \quad (\text{I.9})$$

where  $\frac{1}{\sqrt{N_e!}}$  is a normalization factor.

## 4- Density Functional Theory (DFT)

The aim behind Density Functional Theory (DFT) is to rewrite the Hamiltonian of the electron using electron density rather than wave functions. Researchers like Dirac [9], Slater [10], Hohenburg, and Kohn [11] have made significant contributions to this theory through their theoretical work.

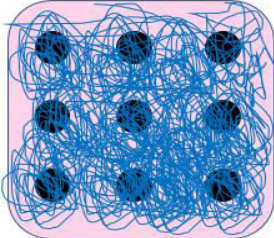
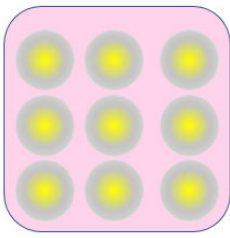
The DFT theory was first discovered in the works of Thomas and Fermi in 1927[13,4], where They originated the core concept of expressing the total energy of an electronic system as a function of electron density by treating the electronic system as a homogeneous and regular gas of electrons where the continuous partitioning of the Brillouin zone (without taking into consideration the correlation between electrons) was executed by the scientists Thomas and Fermi, aiming to establish regions where the electron density remains constant in each part. The subsequent two formulas present expressions for the density and kinetic energy of a homogeneous electronic gas:

$$\rho = \frac{1}{3\pi^2} E_f^{\frac{3}{2}} \left( \frac{2m_e}{h^2} \right)^{\frac{3}{2}} \quad (\text{I.10})$$

$$E_c = \frac{3}{5} \left( \frac{h^2}{2m_e} \right) (3\pi^2)^{\frac{2}{3}} \rho^{\frac{5}{2}} \quad (\text{I.11})$$

The ensuing table provides a comparative analysis between the Hartree-Fock method and density functional theory, elucidating the distinctive characteristics in each method.[3].

**Table I. 1:** Comparison between the two methods, Hartree-Fock and the Density Functional Theory (DFT) [14,15].

HF method	DFT
<div style="text-align: center;"> <math>\Psi(\mathbf{r})</math>   </div>	<div style="text-align: center;"> <math>E[\rho(\mathbf{r})]</math>   </div>
<ul style="list-style-type: none"> <li>• Principle: Schrödinger equation is solved by considering the wave functions as a variable basic.</li> <li>• Depended on the theory of the mean field theory (MFT).</li> <li>• Calculates wave functions and eigenvalue energy to obtain ground state energy.</li> <li>• Depend on the large number of variables, which makes the equation very complicated and time consuming.</li> <li>• The wave functions obtained as solutions for the Schrödinger equation have no physical meaning.</li> <li>• Does not take into account the correlation terms.</li> </ul>	<ul style="list-style-type: none"> <li>• Principle: Solving the Schrödinger equation by considering the electron density as a variable basic.</li> <li>• Based on the two Hohenburg – Sham theorems and shifting from the Schrödinger equation to the Kohn-Sham equations to find the solution.</li> <li>• Use electron density which has physical meaning.</li> <li>• Reduce the number of variables which makes the equation simpler and faster compared to the HF method.</li> <li>• Used to treat the correlation terms.</li> </ul>

## 4-1 Formalism of Density Functional Theory (DFT)

Density functional theory (DFT) is founded on the concept of expressing the overall energy of a system containing numerous interacting electrons in terms of electronic density, rather than wave function, where the electronic density is expressed by the formula:

$$\rho(\vec{r}) = \sum_{i=1}^N |\psi_i(\vec{r})|^2 \quad (\text{I.12})$$

The Density Functional Theory (DFT) is based on two main theorems:

### I. Hohenberg and Kohn Theorems

The foundational principles of density functional theory are encapsulated in the two theorems introduced by Hohenberg and Kohn in 1964, which fundamentally revolutionized our understanding of quantum mechanics by establishing a framework that describes the electronic structure of many-body systems solely in terms of the electron density distribution, rather than the more complex and computationally intensive wave function.



#### A-1) First theorem:

The total energy of an electronic system is a functional of the electron density for an external potential  $V(r)$ , so it is possible to know all the properties of the system when determining the electron density[3,16].

$$E[(\vec{r})] = F[(\vec{r})] + \int V(\vec{r})(\vec{r})dr^3 \quad (\text{I.13})$$

Where  $F[\rho]$  is universal functional.

The external potential and the universal functional  $F[\rho]$  are expressed in the form:

$$V_{ext}(\vec{r}_i) = -\sum_A \frac{Z_A}{r_{iA}} \quad (\text{I.14})$$

$$F[\rho] = T[\rho] + U[\rho] \quad (\text{I.15})$$

Where  $Z_A$  is the charge of the nucleus,  $r_{iA}$  is the distance between nucleus A and electron i.

**A-2) Second theorem:**

The second theory states that in order to derive the total energy of the ground state of the electronic system, one only needs to identify the electron density that minimizes the density function.

$$E(\rho_0(\vec{r})) \leq E[\rho(\vec{r})] \quad (\text{I.16})$$

$$E(\rho_0) = \text{Min}E(\rho) \lim_{\rho \rightarrow N} \langle \Psi | \hat{T} + \sum_i V_{ext} + V_{ee} | \Psi \rangle \quad (\text{I.17})$$

We can get the corresponding electron density of the ground state, by applying the variational principle via the differential of total energy in terms of electron density:

$$\frac{dF[\rho(r)]}{d\rho(r)} + V(r) = 0 \quad (\text{I.18})$$

Therefore, if the electron density which minimizes the energy function is known, we can easily determine the wave function and the exact energy of the ground state.

**II. The Kohn - Sham equation**

One of the difficulties in studying a many-electrons system is the inability to express the kinetic energy and electron-electron interactions analytically in terms of electron density.

In 1965, Scientists Kohn and Sham proposed the foundational concept of substituting the actual electronic system with a fictive system, where in the behavior of each electron is independent, unrelated, and unaffected by the actions of other electrons. It is only affected by the effective potential (Kohn-Sham potential). This entails considering both the external potential generated by the influence of the nuclei and the potential resulting from the impact of the remaining particles on this specific electron[3,17,18].



The fictive system proposed by Kohn-Sham is characterized by:

- ✓ The Kohn-Sham orbits which are space wave functions of a single electron are solutions of the Schrödinger equation in this vacuum space.
- ✓ The fictive electronic system has the same electronic density as a real system.
- ✓ The kinetic energy of the fictive system is the kinetic energy of the electrons without the correlation effect and it is positive, while the kinetic energy in the real system “ $T_R$ ” is the sum of the kinetic energy of the fictive system “ $T_f$ ” and an additional term that expresses the effect of the correlation “ $T_c$ ” on the kinetic energy of the electron [3] that is:

$$T_R = T_f + T_c \quad (\text{I.19})$$

$$T_c = \langle \Psi | T | \Psi \rangle - \langle \varphi | T_s | \varphi \rangle \quad (\text{I.20})$$

The  $V_{ee}$  interaction between electrons in the real system which is written in the following relation:

$$\langle \Psi | V_{ee} | \Psi \rangle = U_H + U_x + U_c \quad (\text{I.21})$$

where the terms represent:

$U_H$ : The electronic Coulomb (Hartree potential)

$U_x$ : The exchange energy between electrons of the same spin.

$U_c$ : The correlation energy between the electrons.

The Kohn-Sham equation for an electronic system is given as a function of the kinetic energy of the electron: external potential energy, Hartree interaction and exchange-correlation energy as follows:

- ✓ The kinetic energy of an electron in a fictitious system:

$$T_s[\rho] = \left\langle \varphi_i \left| -\frac{\hbar^2}{2m} \Delta \right| \varphi_i \right\rangle = -\frac{\hbar^2}{2m} \sum_i \int \varphi_i \nabla^2 \varphi_i^* dr_i \quad (\text{I.22})$$

- ✓ The external potential generated by the effect of nuclei (nucleus-electron interaction):

$$V_{NE}[\rho] = - \int \sum_{I,i} \frac{Z_I \rho(\vec{r})}{|\vec{R}_I - \vec{r}|} d\vec{r} \quad (I.23)$$

- ✓ The Hartree potential (Coulomb electron-electron interaction)

$$U[\rho] = \frac{1}{2} \int \frac{\rho(\vec{r})\rho(\vec{r}')}{|\vec{r}-\vec{r}'|} d\vec{r}d\vec{r}' \quad (I.24)$$

- ✓ The exchange-correlation energy, which is the sum of the correlation and exchange terms, it does not have an exact mathematical expression, but it is estimated by approximations

$$E_{xc}[\rho] = E_x[\rho] + E_c[\rho] \quad (I.25)$$

And finally, the Kohn-Sham equation is written as follows [19–21]:

$$H_{KS}\varphi_i(\vec{r}) = [T_s[\rho] + V_{KS}(\vec{r})]\varphi_i(\vec{r}) = \varepsilon^{KS}\varphi_i(\vec{r}) \quad (I.26)$$

$$V_{KS}(\vec{r}) = V_{ext}(\vec{r}) + V_H(\vec{r}) + V_{XC}(\vec{r}) \quad (I.27)$$

$$E[\rho] = T_s[\rho] + V_{NE}[\rho] + U_H[\rho] + E_{xc}[\rho] \quad (I.28)$$

## 1- Solution of the Kohn - Sham Equation

Solving the Kohn-Sham equation depends on two basic steps:

- The first step: define all the terms of the effective Kohn-Sham potential. the exchange-correlation potential  $E_{xc}$  must be determined because this term has no mathematical formula but it can be estimated by approximations.
- The second step: find the wave functions (Kohn-Sham orbits), which represent a solutions for the Kohn-Sham equation given by [3]:

$$\varphi_{KS}(\vec{r}) = \sum_j C_{ij} \varphi_j(\vec{r}) \quad (I.29)$$

Where  $\varphi_i(\vec{r})$  are the basic functions, and  $C_{ij}$  are are the development coefficients.

$$\sum_j C_{ij} H_{KS} |\varphi_j\rangle = \sum_j C_{ij} \varepsilon_{KS} |\varphi_j\rangle \quad (I.30)$$

$$\langle \varphi_k | \sum_j C_{ij} H_{KS} |\varphi_j\rangle = \langle \varphi_k | \sum_j C_{ij} \varepsilon_{KS} |\varphi_j\rangle \quad (I.31)$$

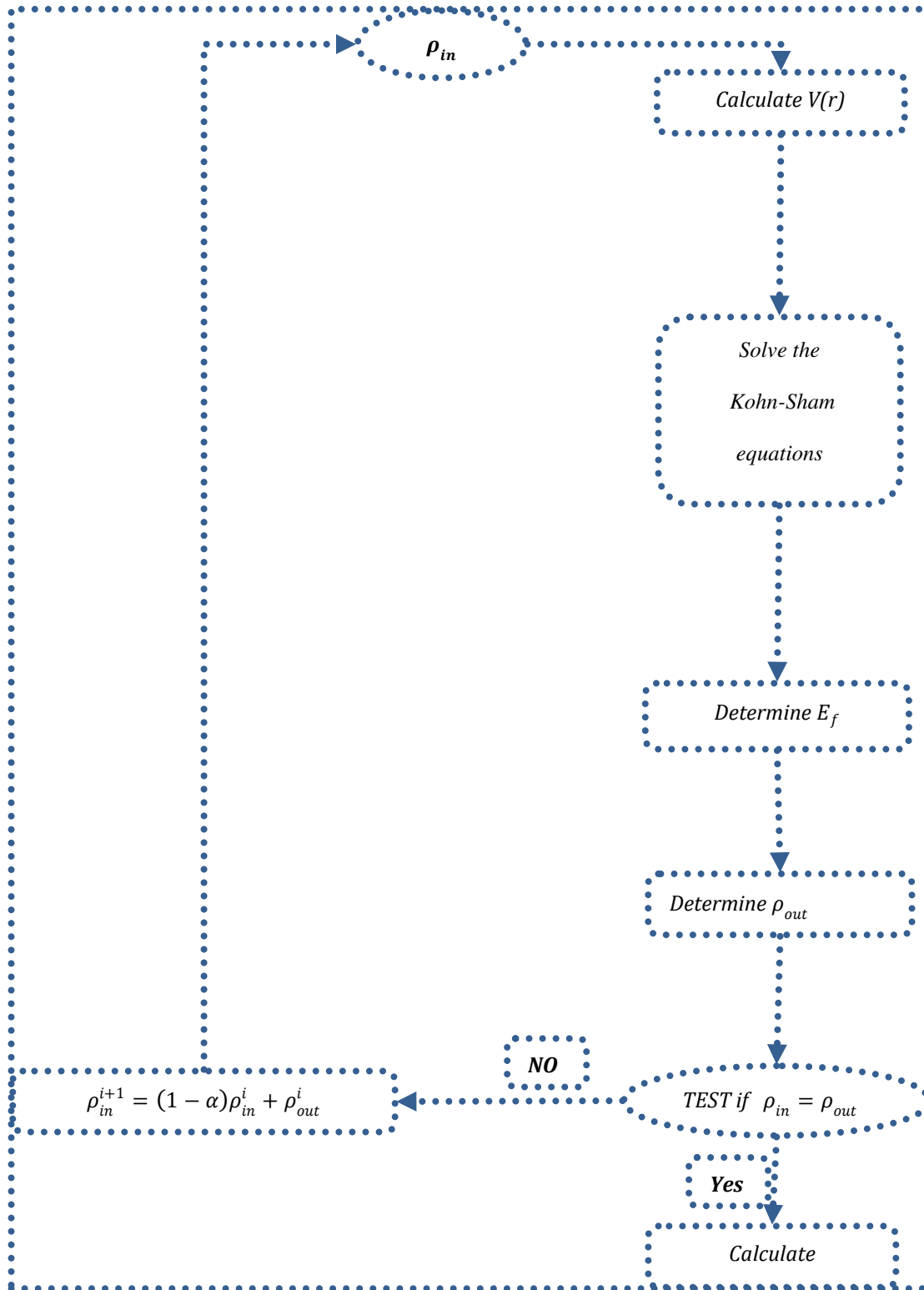
$$\sum_j (\langle \varphi_k | H_{KS} |\varphi_j\rangle - \varepsilon_{KS} \langle \varphi_k | \varphi_j \rangle) C_{ij} = 0 \quad (I.32)$$

It remains to determine the  $C_{ij}$  coefficients.

The Kohn-Sham equation is solved according to an iterative cycles illustrated by figure (I.1), where the process starts using an initial density  $\rho_{in}$  for the first iteration, this density is used to solve the Kohn-Sham equation, then, We use a superposition of the atomic densities and we compute the Kohn-Sham matrix, to solve the equations to obtain the Kohn-Sham orbitals. After this step, we calculate the new density  $\rho_{out}$ , to check the convergence condition (if the density or energy has changed a lot or not) and we mixed the two charge densities  $\rho_{out}$  and  $\rho_{in}$  as follow:

$$\rho_{in}^{i+1} = (1 - \alpha) \rho_{in}^i + \rho_{out}^i \quad (I.33)$$

Thus the iterative procedure can be repeated until the convergence condition is fulfilled.

**Figure I. 1:** Self-consistent calculation flowchart.

## 5-The Different Types of Approximation of the $E_{xc}[\rho]$

Since there is no analytical expression for the exchange-correlation potential between electrons, various approaches have been employed to approximate its values. The precision of the results obtained is primarily contingent on the mathematical formulation chosen for this potential[3].

### 5-1 Local density approximation (LSDA)

This local density approximation (LSDA) was first proposed by Kohn and Sham in 1964 [22] where the inhomogeneous electronic system is approximated by a local homogeneous electronic system after dividing the Brillouin region into small regions, and the expression energy exchange - correlation is given by the relation :

$$E_{XC}^{LSDA} = \int \rho(\vec{r}) E_{xc}[\rho(\vec{r})] d\vec{r} \quad (I.34)$$

$$V_{xc} = \frac{dE_{XC}^{LDA}[\rho]}{d\rho} = \varepsilon_{XC}^{LDA} + \rho(\vec{r}) \frac{d\varepsilon_{XC}^{LDA}}{d\rho} \quad (I.35)$$

For each spin up or down magnetic order, the total electron density becomes the sum of the two electron densities

$$\rho(\vec{r}) = \rho_{\uparrow}(\vec{r}) + \rho_{\downarrow}(\vec{r}) \quad (I.36)$$

The Kohn-Sham equation for the two spins in the form [3]:

$$\left\{ \begin{array}{l} \left( \frac{-\hbar^2}{2m} \nabla^2 + V_{eff}^{\uparrow}(\vec{r}) \right) \varphi_i(\vec{r}) = \varepsilon_{KS}^{\uparrow} \varphi_i(\vec{r}) \\ \left( \frac{-\hbar^2}{2m} \nabla^2 + V_{eff}^{\downarrow}(\vec{r}) \right) \varphi_i(\vec{r}) = \varepsilon_{KS}^{\downarrow} \varphi_i(\vec{r}) \end{array} \right. \quad (I.37)$$

### 5-2 The Generalized Gradient Approximation GGA

The Generalized Gradient Approximation GGA is a new approximation was developed, in which the localized electron density was considered to be non-homogeneous and varied from place to place. so, the total energy of the electron system is proportional to both the electron density  $\rho(\vec{r})$  and its gradient  $\nabla\rho(\vec{r})$ , as shown by the equation[23]:

$$E_{XC}^{GGA}[\rho(\vec{r})] = \int d^3\vec{r} \rho(\vec{r}) \epsilon_{XC}[\rho(\vec{r}), \nabla\rho(\vec{r})] \quad (I.38)$$

## 6- Full-Potential Linearized Augmented Plane-wave Method FP-LAPW

this method aimed to look for the wave functions as solutions to the Kohn-Sham equation became necessary. After extensive research, certain approaches emerged, including the OPW method presented by Herring theory in 1940 [24], the LMTO method [25], and the FP-LAPW method, where these methods are dependent on the quality of the effective potential utilized.

### 6-1 The Plane Wave method (APW)

The plane wave method was carried out by the scientist Slater [26] where he divided the crystal space into two parts based on the Muffin-Tin approximation [27] (see Figure I.2) by representing the atoms as non-overlapping spheres of radius  $R_0$  in which the core electrons are located, and between these spheres, an interstitial region containing free electrons that are away from the nuclei of their atoms.

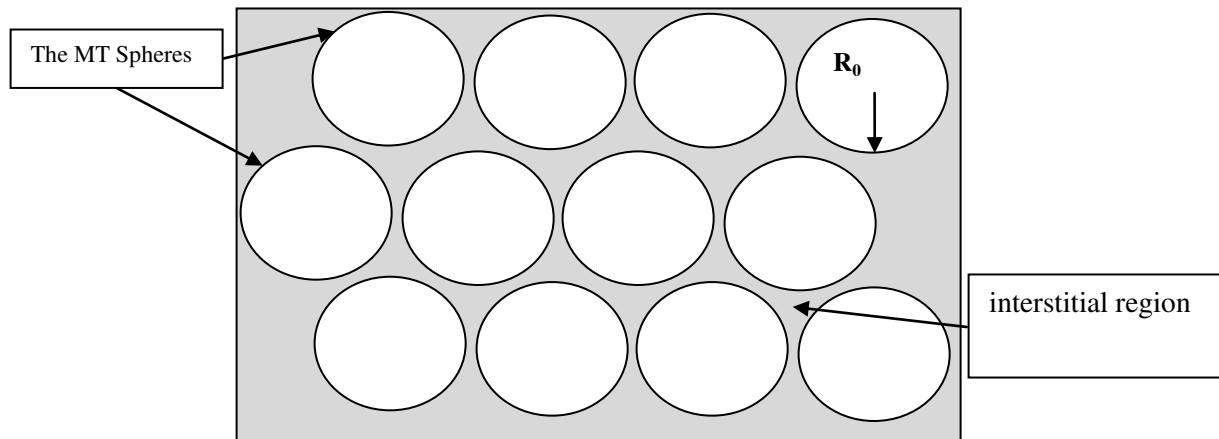


**Figure I. 2:** Diagram of the distribution of the elementary cell in atomic spheres and in interstitial region.

According to this approximation, the core electrons located inside the sphere are subjected to the spherical potential, on the other hand, in the interstitial region the potential is constant [3]. So, the potential in the two regions is given in the form:

$$V(\vec{r}) = \begin{cases} V(r) & r \leq R_0 \\ 0 & r > R_0 \end{cases} \quad (I.39)$$

The waves that describe the behavior of electrons inside MT spheres differ from those in the interstitial region, they are described by plane waves in the interstitial region, while inside spheres by functions radials multiplied by spherical harmonics[3]. The two different wave functions are given by the following expression:

$$\varphi(\vec{r}) = \begin{cases} \sum_{l=0}^{\infty} \sum_{-m}^m A_{lm} U_l(r) Y_{lm}(r) & r \leq R_0 \\ \frac{1}{\sqrt{\Omega}} \sum_G C_G e^{i(\vec{K}+\vec{G})\vec{r}} & r > R_0 \end{cases} \quad (I.40)$$

Where ,  $\Omega$ : The cell volume

$Y_{lm}$ : Spherical harmonics

$A_{lm}$ : Development coefficients

$U_l$ : The regular solution of the Schrödinger equation given by[28]:

$$\left( -\frac{d^2}{dr^2} + \frac{l(l+1)}{r^2} V(\vec{r}) \right) r U_l = E_l U_l \quad (I.41)$$

Where  $E_l$ : An energy parameter.

## 6-2 The Linearized Augmented Plane Wave Method (FP-LAPW)

The darkpoint of using the APW method is its slow process in calculations due to the common radial function  $U_l$ ; additionally, it is difficult to define the radial function for each value of energy  $E_l$ . so that, Anderson [29]made improvements to the APW method [30]by using the Taylor expansion to write the radial functions  $U_l(r)$  in the following form:

$$U_l(r, E) = U_l(r, E_l) + (E_l - E) \left. \frac{dU_l(r, E)}{dE} \right|_{E=E_l} + \mathcal{O}(E_l - E)^2 \quad (I.42)$$

Where the term  $\mathcal{O}(E - E_l)^2$  represents the quadratic error.

After several simplifications, he has got the expression of potential inside and outside of Muffin-Tin balls as follows:

$$V(r) = \begin{cases} \sum_{lm}^m V_{lm}(r) Y_{lm} & r \leq R_0 \\ \sum_{lm}^m V_k(r) e^{ikr} & r > R_0 \end{cases} \quad (I.43)$$

As well as the wave functions inside the spheres in terms of radial functions and their derivatives. Where the wave functions are written as follows [31,32]:

$$\Phi_{\vec{K}+\vec{G}}(\vec{r}) = \begin{cases} \sum_{lm} (A_{lm} U_l(r) + B_{lm} \dot{U}_l(r)) Y_{lm}(r) & r \leq R_0 \\ \frac{1}{\sqrt{\Omega}} \sum_G C_G e^{i(\vec{K}+\vec{G})\vec{r}} & r > R_0 \end{cases} \quad (I.44)$$

Where :

$\vec{K}$ : represents the wave vector.

$\vec{G}$  : is the vector of the reciprocal lattice.

$A_{lm}$ :: are coefficients corresponding to the function  $U_l$ .

$B_{lm}$ : are coefficients corresponding to the function  $U_l$ .

We can determine the coefficients  $A_{lm}$  and  $B_{lm}$ , for each wave vector, and for each atom by applying the conditions of continuity of the basic functions in the vicinity of the limit of the spheres. After some simplifications we find the coefficient formula  $A_{lm}$  and  $B_{lm}$  in the following forms:

$$A_{lm} = \frac{4\pi r_0^2 i^L}{\sqrt{\Omega}} Y_{lm}^*(K+G) a_l(K+G) \quad (I.45)$$

$$B_{lm} = \frac{4\pi r_0^2 i^L}{\sqrt{\Omega}} Y_{lm}^*(K+G) b_l(K+G) \quad (I.46)$$

## 7- WIEN2K software

This program consists of many subprograms written in Fortran language, which are algorithms that translate equations of the crystalline system processed according to density functional theory (DFT), adopting the full potential linearized augmented plane wave (FP-LAPW) method as a means to calculate algorithms for studying compound properties [3].

The most important subprograms and their roles in the Wien2k program[33] are indicated in the diagram presented in Figure I.3 and are organized as follows: [3]:

- ❖ NN: This subprogram calculates distances between nearest neighbors up to a specified limit, thus helping to determine the value of the atomic sphere radius.
- ❖ SGROUP: Determines the space group of the compound.
- ❖ SYMMETRY: A program that determines the symmetry number and symmetry operations of the space group of our structure.
- ❖ LSTART: Computes electron densities of free atoms and determines how different orbitals will be treated in band structure calculations.
- ❖ KGEN: Generates a mesh of K points in the irreducible part of the first Brillouin zone (1st BZ). The number of K points in the entire 1st BZ is specified.
- ❖ DSTART: Produces an initial density for the self-consistent field (SCF) cycle by superimposing atomic densities produced in the LSTART subprogram.

After the last subprogram, we enter into a loop of SCF calculations and consequently proceed to the following five steps:

- ✓ LAPW0 (POTENTIAL): Uses the total electron density to calculate the Coulomb and exchange potentials (Hartree-Fock potential). Additionally, it divides space into a muffin-tin (MT) sphere and an interstitial region.
- ✓ LAPW1 (BANDS): Calculates eigenvalues and wave functions for valence electrons from the solution of equation (I.1) .
- ✓ LAPW2 (RHO): Calculates valence electron densities obtained in the LAPW0 step.

- ✓ LCORE: Computes eigenvalues and wave functions to obtain core electron densities.
- ✓ MIXER: Computes the new density through mixing.

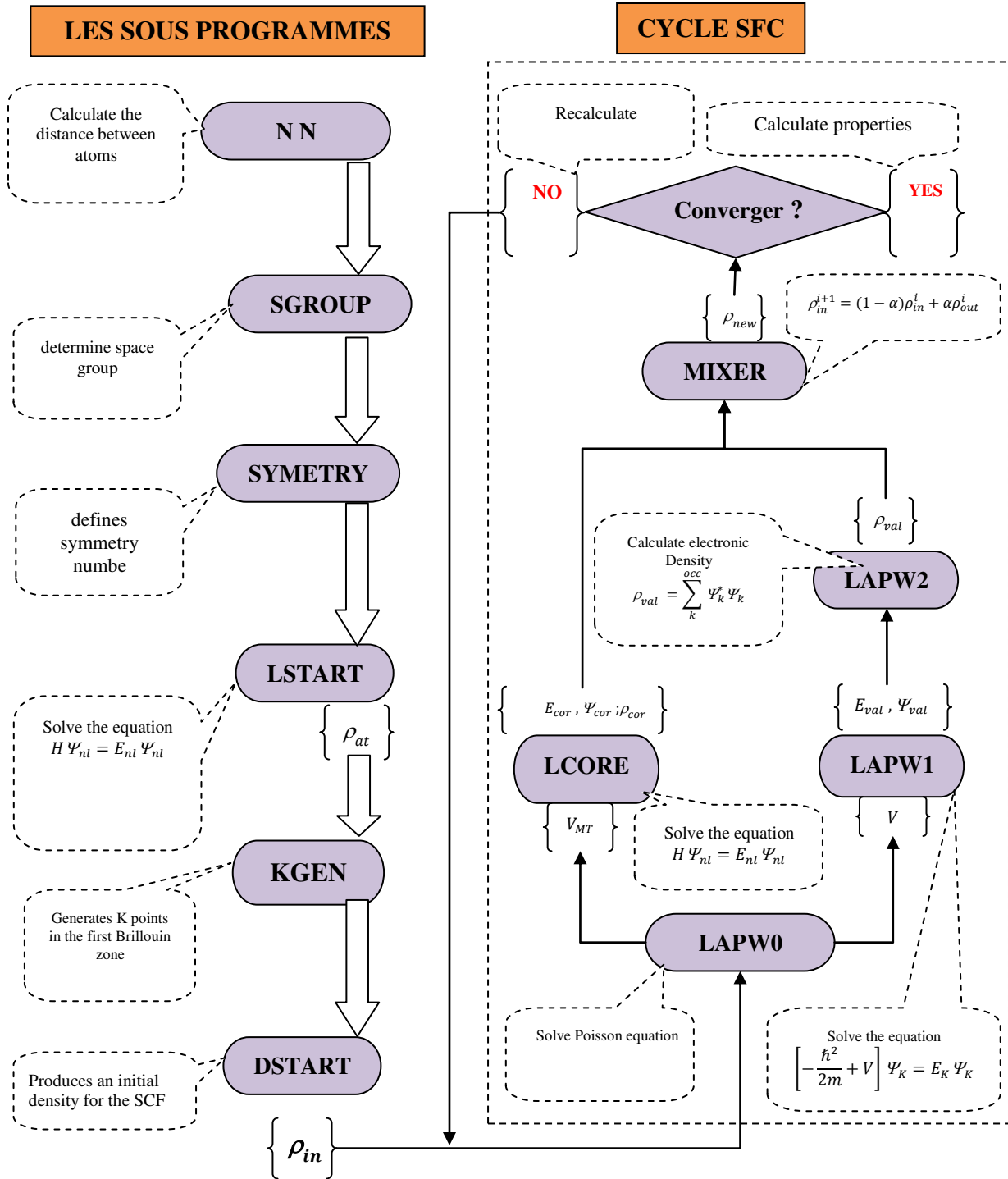


Figure I. 3: The flowchart of the Wien2k code subroutines [3].

## 8- References

- [1] E SCHROEDINGER *Ann. Phys.* (1926).
- [2] S S Essaoud, M Imadalou, and D E Medjadi *Int J Mod. Theo Phys.* **5** 8 (2016).
- [3] S Saad Essaoud *DOCTORAT THESIS* (2020).
- [4] S Saad Essaoud (2013).
- [5] M Born and R Oppenheimer *Ann. Phys.* **389** 457 (1927).
- [6] D R Hartree *The wave mechanics of an atom with a non-coulomb central field. Part II. Some results and discussion* (Cambridge University Press) p 111 (1928).
- [7] D R Hartree *The wave mechanics of an atom with a non-coulomb central field. part iii. term values and intensities in series in optical spectra* (Cambridge University Press) p 426 (1928).
- [8] G Shadmon and I Kelson *Nucl. Phys. A* **241** 407 (1975).
- [9] P A M Dirac *Math. Proc. Camb. Philos. Soc.* **26** 376 (1930).
- [10] J C Slater *Phys. Rev.* **81** 385 (1951).
- [11] P Hohenberg and W Kohn *Phys. Rev.* **136** B864 (1964).
- [12] L H Thomas *Math. Proc. Camb. Philos. Soc.* **23** 542 (1927).
- [13] E Fermi *Z. Für Phys.* **48** 73 (1928).
- [14] Maroua *Master Thesis* (UNIVERSITE MOHAMED BOUDIAF-M'SILA) (2021).
- [15] Koraichi *Master Thesis* (UNIVERSITE MOHAMED BOUDIAF-M'SILA) (2021).
- [16] R M Dreizler and E K U Gross (1990).
- [17] R Stowasser and R Hoffmann *J. Am. Chem. Soc.* **121** 3414 (1999).
- [18] A Seidl, A Görling, P Vogl, J A Majewski, and M Levy *Phys. Rev. B* **53** 3764 (1996).
- [19] C Fiolhais, F Nogueira, and M A Marques *A primer in density functional theory* (Springer Science & Business Media) (2003).
- [20] F M Bickelhaupt and E J Baerends *Rev. Comput. Chem.* **15** 1 (2000).
- [21] J A Pople, P M Gill, and B G Johnson *Chem. Phys. Lett.* **199** 557 (1992).
- [22] W Kohn and L J Sham *Phys. Rev.* **140** A1133 (1965).
- [23] D M Ceperley and B J Alder *Phys. Rev. Lett.* **45** 566 (1980).
- [24] C Herring *Phys. Rev.* **57** 1169 (1940).

- [25] H L Skriver *The LMTO Method: Muffin-Tin Orbitals and Electronic Structure* (Berlin Heidelberg : Springer-Verlag) (1984).
- [26] J C Slater *Phys. Rev.***51** 840 (1937).
- [27] O K Andersen and T Saha-Dasgupta *Phys. Rev. B***62** R16219 (2000).
- [28] D D Koelling and G O Arbman *J. Phys. F Met. Phys.***5** 2041 (1975).
- [29] O K Andersen *Phys. Rev. B***12** 3060 (1975).
- [30] M Petersen, F Wagner, L Hufnagel, M Scheffler, P Blaha, and K Schwarz *Comput. Phys. Commun.***126** 294 (2000).
- [31] D R Hamann *Phys. Rev. Lett.***42** 662 (1979).
- [32] M Weinert *J. Math. Phys.***22** 2433 (1981).
- [33] P. Blaha, K. Schwarz, G. Madsen, D. Kvasnicka, J. Luitz (2001).

## **CHAPTER 2:**

### ***RESULTS AND DISCUSSION***

---

1) Introduction.....	27
2) Calculation Details.....	27
3) Results and discussions.....	28
3-1) Structural properties .....	28
3-2) Electronic Properties.....	33
3-2-1) Energy Bands .....	33
4) The Thermodynamic Properties.....	38
4-1) Heat Capacities .....	38
4-2) Entropy .....	40
4-3) Thermal Expansion Coefficient.....	42
5) thermoelectric Properties .....	44
5-1) Seebeck Coefficient.....	44
5- 2) Electrical Conductivity .....	46
5-3) Electronic Thermal Conductivity .....	47
5-4) ZT Factor .....	49
6) References.....	51

## 1) Introduction

As an application of what was discussed in the theoretical part, we initially studied the structural properties of  $\text{MgSnO}_3$  and  $\text{CaSnO}_3$  perovskite compounds. We calculated the lattice constant as well as the bulk modulus, and its the first derivative. Then, we determined the electronic behavior of the compounds through the analysis of band structure curves and density of states. Finally, we calculated the thermal and thermoelectric properties of the compounds.

## 2) Calculation Details:

The findings in this study were obtained using the linearly augmented plane wave (FP-LAPW) method[1–6], integrated into the Wien2K simulation program [7], primarily based on density functional theory [8–13]. We used only the generalized gradient approximation (GGA) [14] to approximate the exchange-correlation term in estimating structural, electronic, and thermoelectric properties.

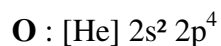
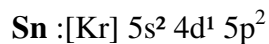
Thermoelectric transport properties are evaluated using the BoltzTraP software[15] that based on the semi-classical Boltzmann theory , whilst the effect of temperature and pressure on heat capacity, Debye temperature lattice thermal expansion and entropy properties have estimated using the quasi-harmonic approximation integrated in GIBBS2 software[16,17].

Based on the muffin-tin (MT) approximation [18], we divided space into two regions:

**First Region:** In this region, we considered atoms as spheres with semi-radii  $R_{\text{mt}}$ , where the wave function inside is described by spherical harmonics with a maximum angular momentum of  $l_{\text{max}}= 10$ . For the compounds we studied, we took the values of 2.0 a.u for each of the "Ca" and "Mg" atoms, 2.0 a.u for the "Sn" atom, and 1.4 a.u for the "O" atom as the semi-radii for the constituent atoms of the compounds. It's important to note that all inner electrons "core electrons" must be contained within these spheres without any overlap between them.

**Second Region:** This intermediate region represents the remaining space from the first region. In this region, the wave function is represented as plane waves with a cutoff parameter  $R_{\text{mt}}K_{\text{max}}$ , where  $R_{\text{mt}}$  is the average muffin-tin radius and  $K_{\text{max}}$  is the maximum value of the wave vector for the reciprocal lattice. The optimal value for the cutoff parameter was chosen

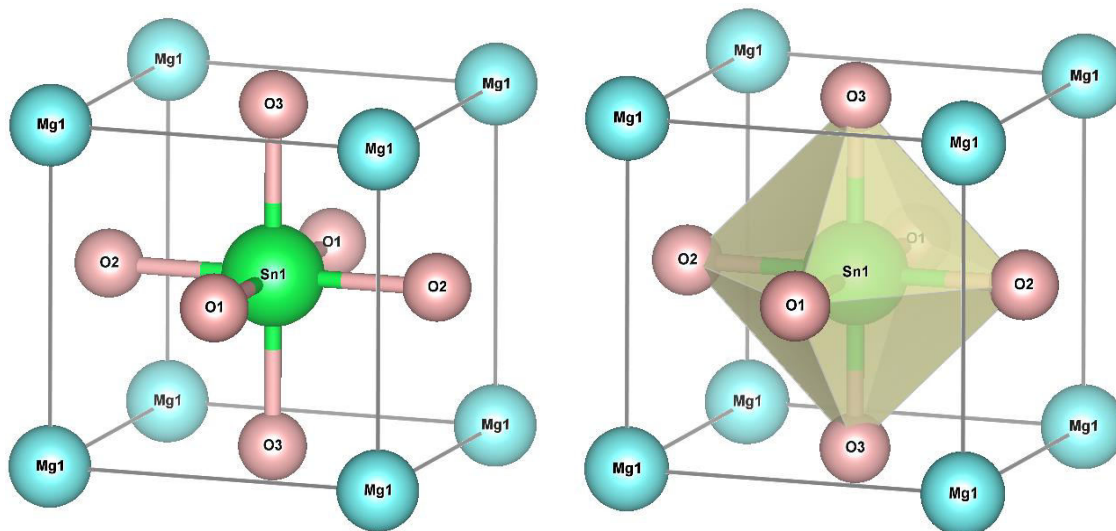
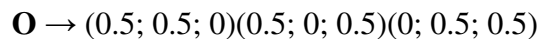
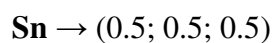
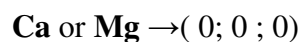
as  $R_{mt}K_{max} = 8$ , with a total of  $k_{-points}=800$  k. The electronic distribution for the constituent atoms of the compounds was as follows

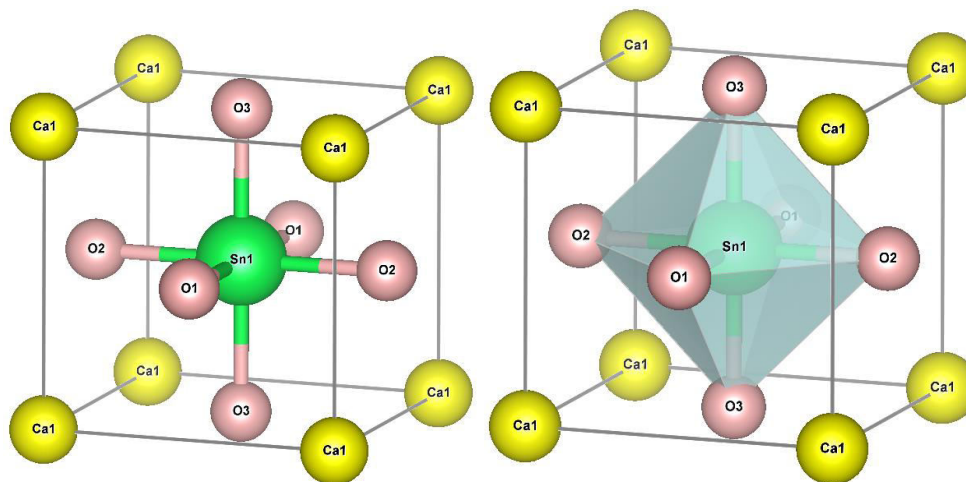


### 3) Results and discussions

#### 3-1) Structural properties

Both compounds  $\text{MgSnO}_3$  and  $\text{CaSnO}_3$ , crystallize in the cubic structure with the space group Pm-3m. The initial unit cell, as depicted using the VESTA program [19–22] and plotted in the FIGURE (II-1), consists of 5 atoms occupying the following Wyckoff positions:





FIGURE( II-1):(a) Crystal structure of  $\text{CaSnO}_3$  and  $\text{MgSnO}_3$ .

to calculate the equilibrium structural properties of the compounds  $\text{MgSnO}_3$  and  $\text{CaSnO}_3$ , we computed the total energy variations for the primitive cell at different volumes using GGA approximations. Subsequently, we plotted the curve of total energy variations as a function of volume and to fit the findings, we employ the Murnaghan equation [23] expressed by the following Equation :

$$E(V) = E_0 + \frac{B}{B'(B' - 1)} \left[ V \left( \frac{V_0}{V} \right)^{B'} - V_0 \right] + \frac{B}{B'} (V - V_0) \quad (II. 1)$$

Where the parameters represent:

- $V_0$  : The volume of the cell at equilibrium.
- $E_0$ : The total energy of the primitive cell at equilibrium.
- $B$ : Bulk modulus.
- $B'$ : Pressure derivative of the bulk modulus.

The expression for the bulk modulus is given by the equation:

$$B = -V \frac{\partial P}{\partial V} = V \frac{\partial^2 E}{\partial V^2} \quad (II. 2)$$

Through the plotted curves presented in FIGURE (II-2), we determined the corresponding volume for the minimum energy. Afterwards, we calculated the lattice constant  $a(\text{\AA})$  and the bulk modulus, comparing them with other results, whether experimental or theoretical, as

illustrated in TABLE (II-1). We observe the obtained results were consistent with those obtained in other works. Regarding the bulk modulus, which reflects the material's resistance to deformation under external pressure, we found that the compound  $\text{MgSnO}_3$  has a larger bulk modulus than the compound  $\text{CaSnO}_3$ . Therefore, it is more resistant to pressure and hence serves as a good indicator of the high stability of both  $\text{MgSnO}_3$   $\text{CaSnO}_3$  and against pressure effect. also, According to the volume change curves as a function of pressure, we observe that the breaking of the crystal lattice decreases almost linearly with increasing pressure.

**TABLE II-1:** Values of the structural parameters obtained for  $\text{MgSnO}_3$  and  $\text{CaSnO}_3$  compounds and calculated by GGA approximation.

<b>MgSnO<sub>3</sub></b>		<b>CaSnO<sub>3</sub></b>	
<b>V<sub>0</sub>(a.u)<sup>3</sup></b>	444.4368	<b>V<sub>0</sub> (a.u)<sup>3</sup></b>	457.3079
<b>B(GPa)</b>	155.5685	<b>B(GPa)</b>	149.2411
<b>BP(GPa)</b>	4.7940	<b>BP(GPa)</b>	4.6621
<b>E<sub>0</sub></b>	-13210.483318	<b>E<sub>0</sub></b>	-14170.841981
<b>Cubic lattice parameter</b>	4.0384 Ang	<b>Cubic lattice parameter</b>	4.0770 Ang

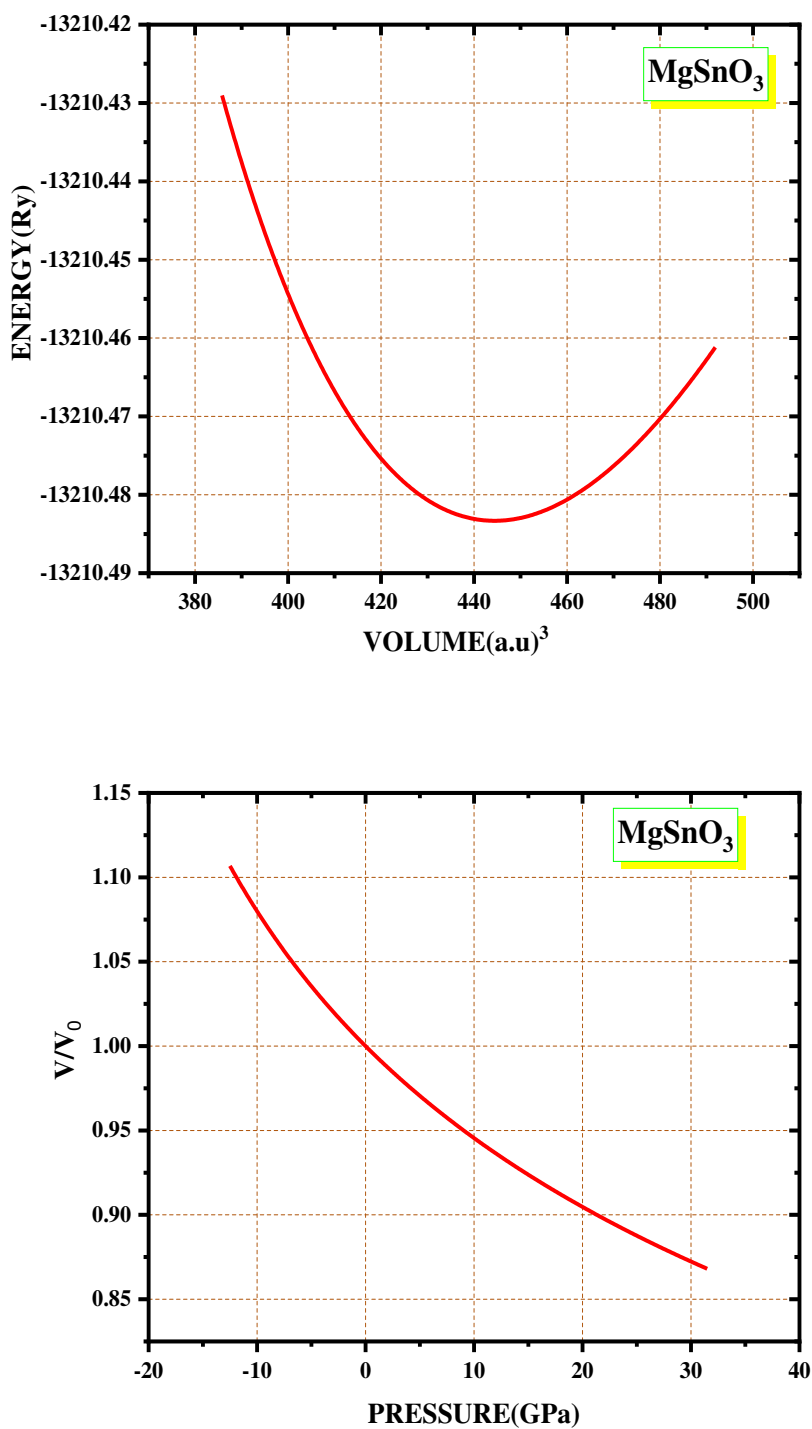


**FIGURE II-2:** Total Energy-Volume and volume-pressure Curves of **MgSnO<sub>3</sub>** calculated using GGA-sol approximations.

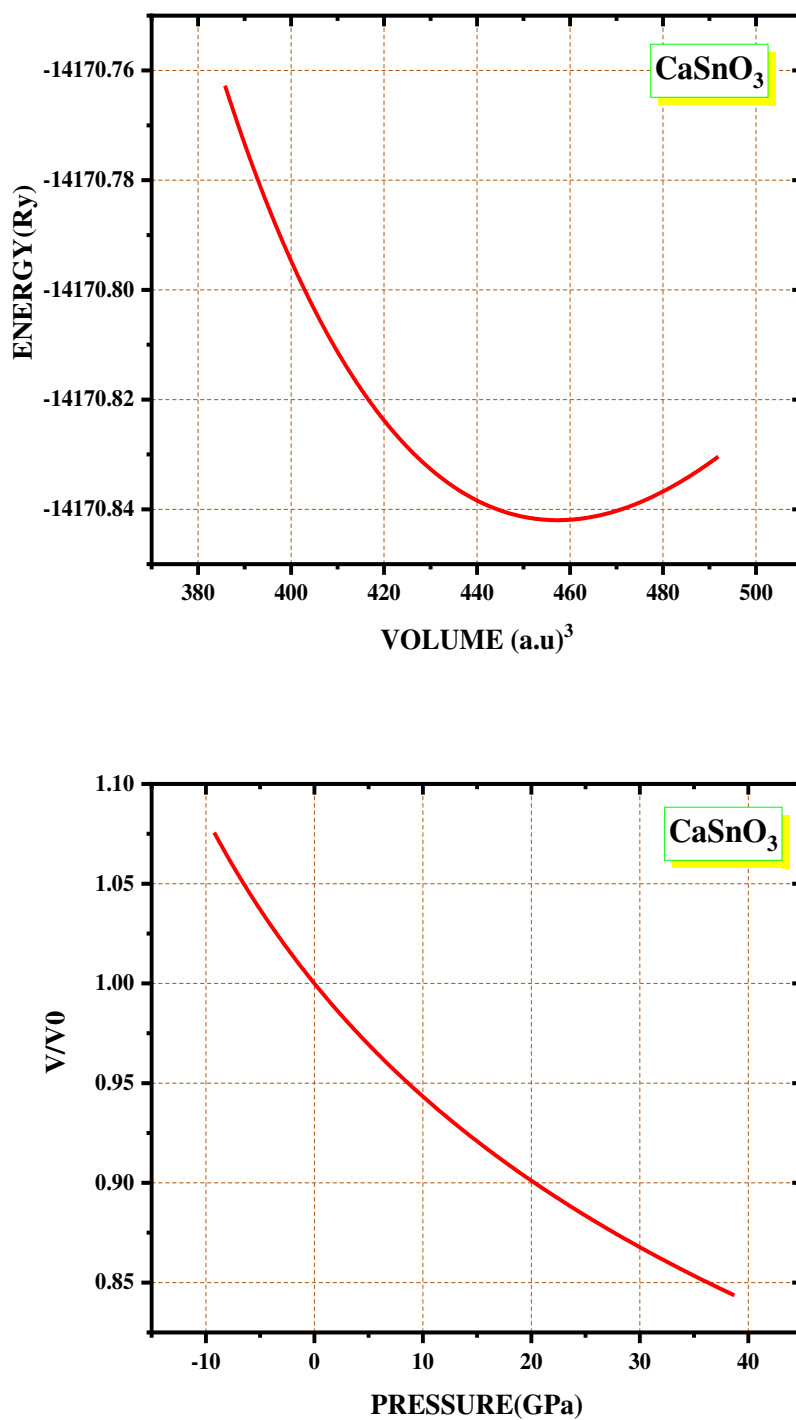


**FIGURE II-3:** Total Energy-Volume and volume-pressure Curves of  $\text{CaSnO}_3$  calculated using GGA-sol approximations.

### 3-2) Electronic Properties:

The investigation of electronic properties holds significant importance as it enables the identification of the most appropriate electronic or electrical applications for a material. This objective is accomplished through a thorough comprehension of the compound's electronic characteristics. Consequently, our research delved into the energy bands of the compounds, aiming to ascertain their electronic behavior; whether they fall into the categories of insulating, conducting, or semi-conducting materials. Additionally, we explored the density of states to pinpoint the atomic orbitals influencing each band, thereby enhancing our understanding of the formation of interatomic bonds.

#### 3-2-1) Energy Bands:

The energy bands for both compounds, MgSnO<sub>3</sub> and CaSnO<sub>3</sub>, were studied in their stable state in the first Brillouin zone, along the high-symmetry points and following the path (R- $\Gamma$ -X-M- $\Gamma$ ).

Through studying the energy band diagrams drawn for both compounds and calculated GGA approximations, we noted the following points:

- ✓ For both compounds: When using both GGA approximations, we observed that there are no energy bands crossing the Fermi level, and there is an energy gap separating the valence bands (below the Fermi level) from the conduction bands (above the Fermi level). Thus, electrons in the valence bands can only transition to the conduction bands if they acquire energy greater than the energy gap value.
- ✓ The value of the energy gap is the difference between the lowest point in the conduction band and the highest point in the valence band.
- ✓ The energy gap value for the CaSnO<sub>3</sub> compound is 1.13 eV (indirect band-gap  $\Gamma$ -M) when using GGA approximations, respectively.
- ✓ The energy gap value for the MgSnO<sub>3</sub> compound is 0.76 eV (indirect band-gap  $\Gamma$ -M) when using GGA approximations, respectively.

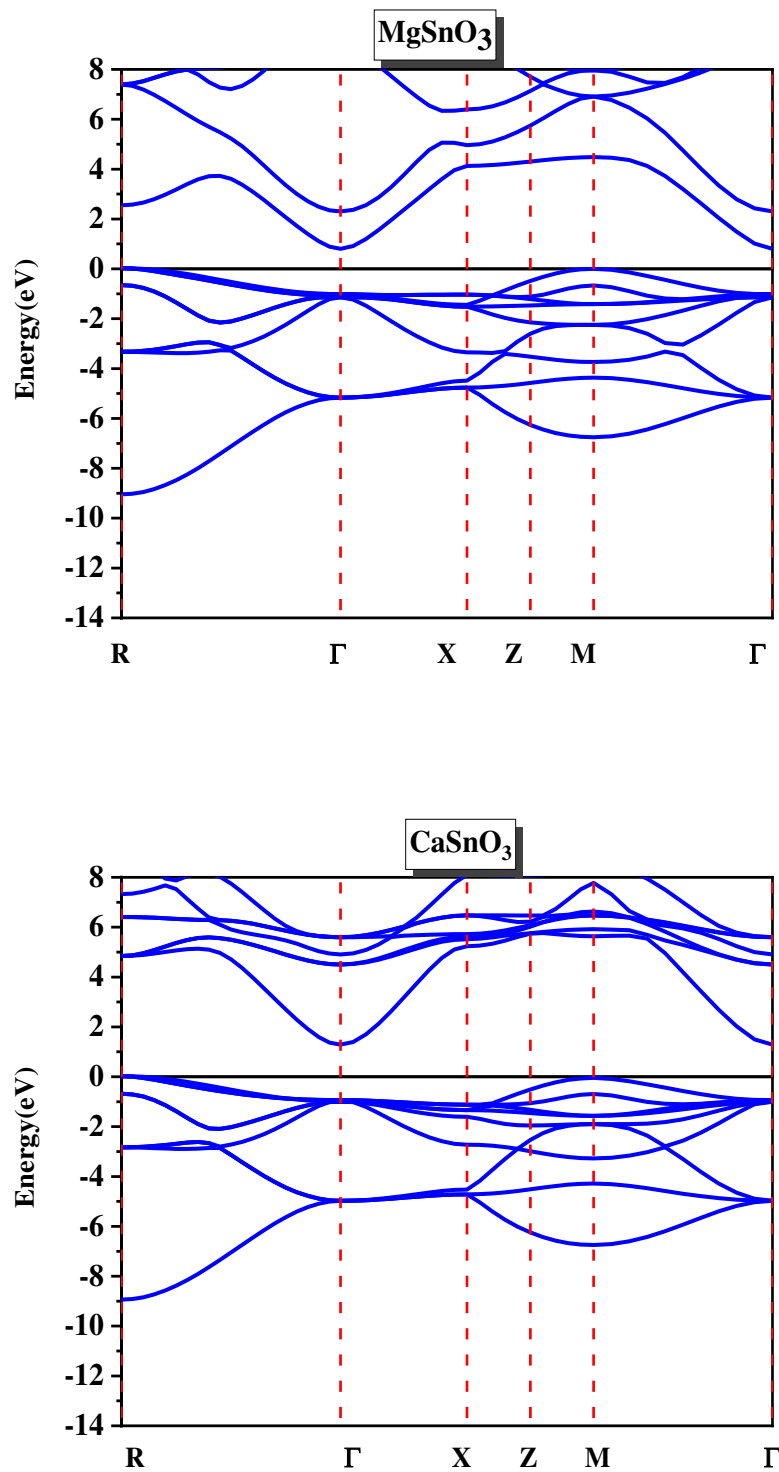


FIGURE II-4: band structure spectra for both compounds MgSnO<sub>3</sub> and CaSnO<sub>3</sub>.

**3-2-2) Total Density of States (TDOS) Partial Density of States (PDOS):**

Understanding which electrons contribute to each energy band and interpreting atomic bond formation often requires a detailed study of a compound's electronic properties. This is typically achieved through analyzing the Total Density of States (TDOS) and partial density of states (PDOS) curves as a function of energy. Figure (II.5) and Figure (II.6) shows the distribution of both the total and partial density of states for the compounds MgSnO<sub>3</sub> and CaSnO<sub>3</sub> calculated using the GGA approximations. Through it, we can record the following observations:

- 1- The absence of states around the Fermi level for both compounds confirms the semiconducting behavior of both compounds.
- 2- For both compounds MgSnO<sub>3</sub> and CaSnO<sub>3</sub>, we obtained identical curves using the GGA approximation. As shown in the figure, The valence and conduction bands are separated by an energy gap with a value equal to that obtained when studying the energy bands.

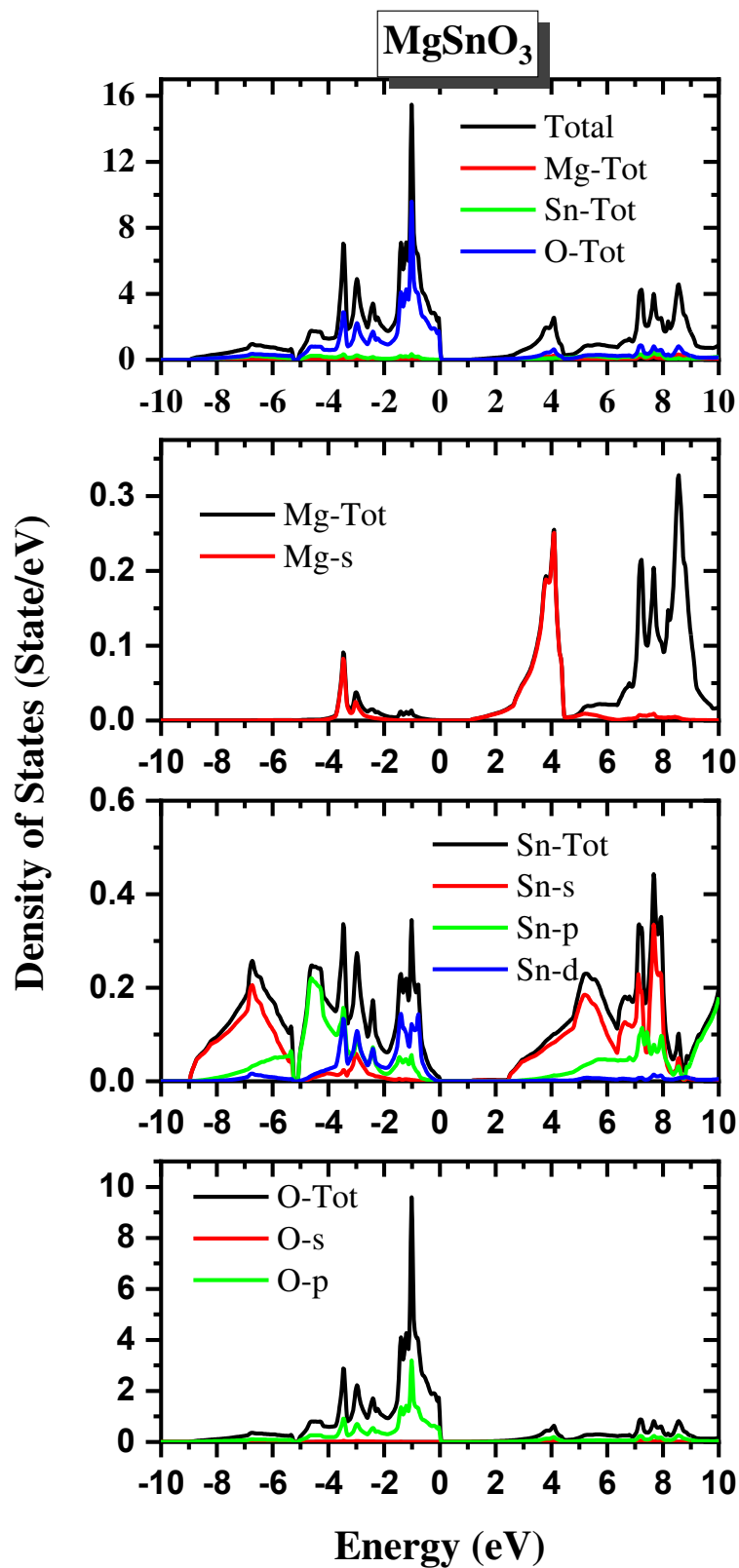
The contributions of atomic orbitals with respect to the energy indicated in Figure (II.5) for the compound MgSnO<sub>3</sub> and Figure (II.6) for the compound CaSnO<sub>3</sub> can be divided into several regions as follows:

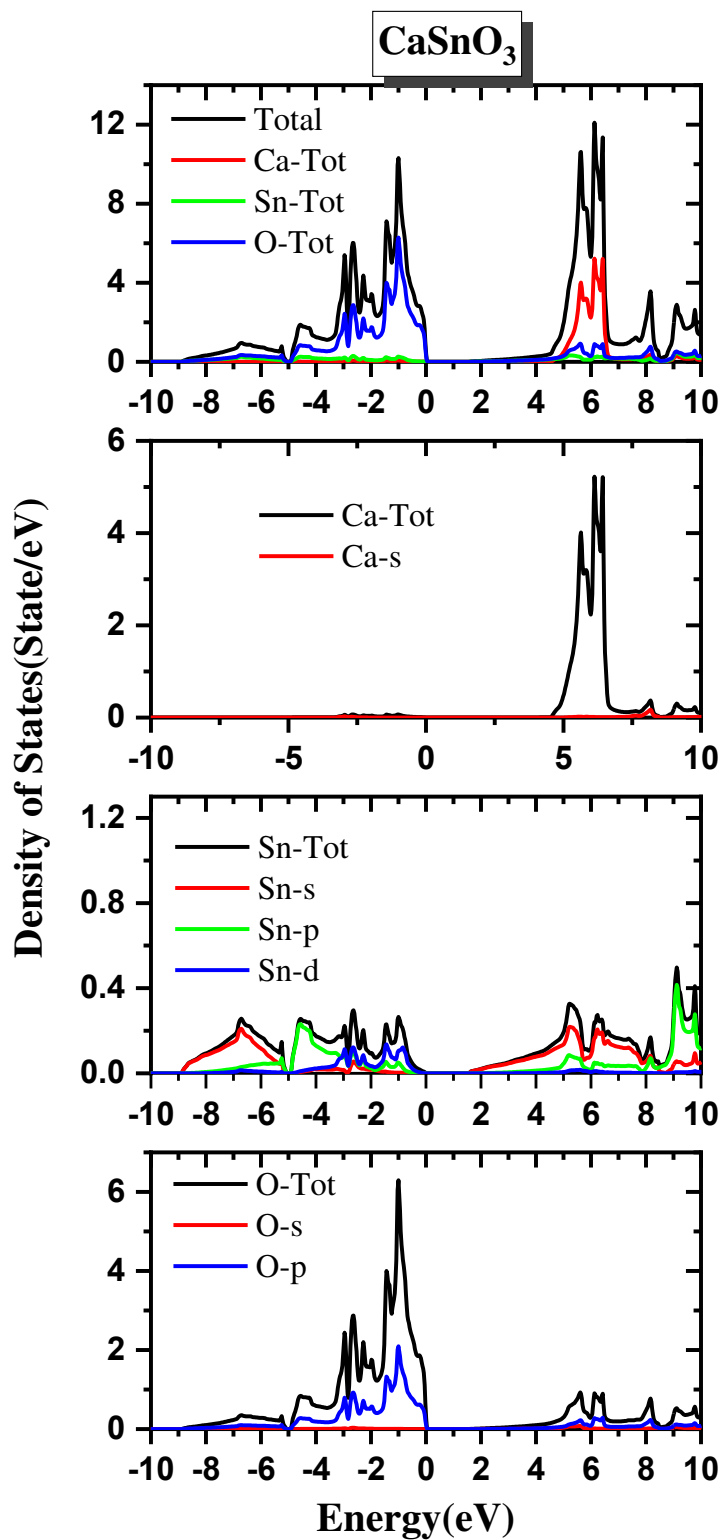
For the compound MgSnO<sub>3</sub> From Figure (II.5), we observe :

- [-9 eV  $\Leftarrow$  -5 eV]: the contribution from the "s" orbital electrons of «Sn » atom.
- [-5 eV  $\Leftarrow$  0 eV]: the contribution from the "p" orbital electrons of «O » atom, "p", and "d" orbital electrons of «Sn » atom.
- [0.7 eV  $\Leftarrow$  8 eV], there is a contribution from the "s" orbital electrons of «Mg »atom, and "s" orbital electrons of «Sn » atom.

.For the compound CaSnO<sub>3</sub> From Figure (II.6), we observe :

- [-9 eV  $\Leftarrow$  -5 eV]: the contribution from the "s" orbital electrons of «Sn » atom.
- [-5 eV  $\Leftarrow$  0 eV]: the contribution from the "p" orbital electrons of «O » atom, "p", and "d" orbital electrons of «Sn » atom.
- [1 eV  $\Leftarrow$  9 eV], there is a contribution from the "s" orbital electrons of «Ca »atom, and "s" orbital electrons of «Sn » atom.

FIGURE II-5: Total and partial density of states of MgSnO<sub>3</sub>.

FIGURE II-6: Total and partial density of states of CaSnO<sub>3</sub>.

## 4- The Thermodynamic Properties

We have dedicated this section to studying some thermal properties of the compounds  $\text{MgSnO}_3, \text{CaSnO}_3$  such as heat capacity at constant pressure or volume, thermal expansion coefficient, entropy, as well as the bulk modulus under the influence of pressure and temperature. Regarding the pressure applied to the substance, our findings are carried out in the pressure range [0-10 GPa], while the effect of temperature was studied in the range [0-800 K].

### 4-1 Heat Capacity $C_v$

The heat capacity of a solid material is a physical quantity that expresses the amount of heat required to raise its temperature by one degree. The heat capacity of any substance is very important because it reflects the material's ability to absorb thermal energy. This ability is primarily related to the number of freedom degrees of the body and the available vibrational modes of its solid-state components. Logically, the absorption capacity increases with an increase in the number of degrees of freedom of the particle[25,26].

After calculating the variation in the heat capacities of the  $\text{MgSnO}_3$  and  $\text{CaSnO}_3$  compounds at constant volume ( $C_v$ ) in response to changes in both temperature and pressure separately, as shown in Figures (II.7) and (II.8) respectively, we observed that the heat capacity  $C_v$  decreases with increasing pressure because the particles approach each other due to the applied pressure on the crystalline lattice, and therefore, the atoms constituting the solid material have less freedom which reducing their ability to absorb energy.

For the temperature dependence of the heat capacity  $C_v$ , we noticed that  $C_v$  increases rapidly with increasing temperature as  $T^3$  at low temperatures (below 200 Kelvin), and then its increase slows down at high temperatures, approaching a limiting value of 125 J/molK according to the Dulong-Petit law[27].

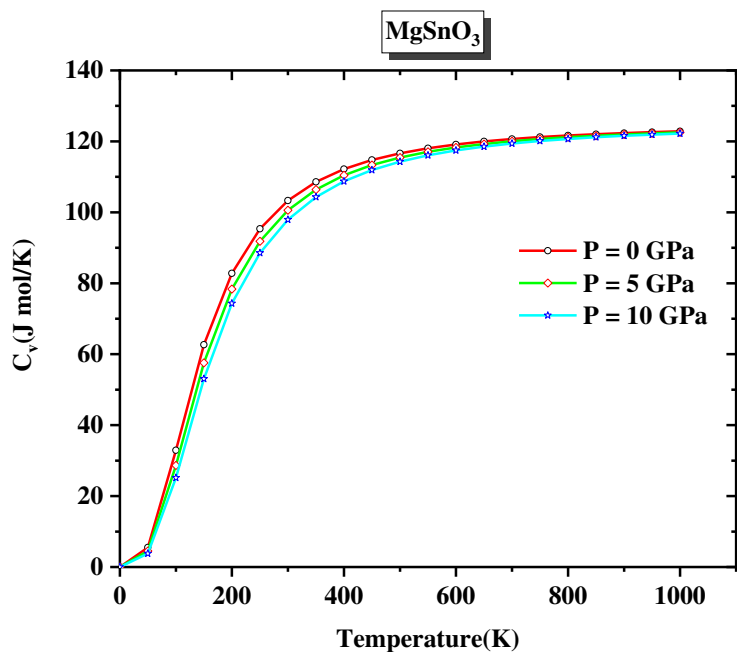


FIGURE II-7: variation of the heat capacity " $C_v$ " of the compound  $MgSnO_3$  as a function of temperature.

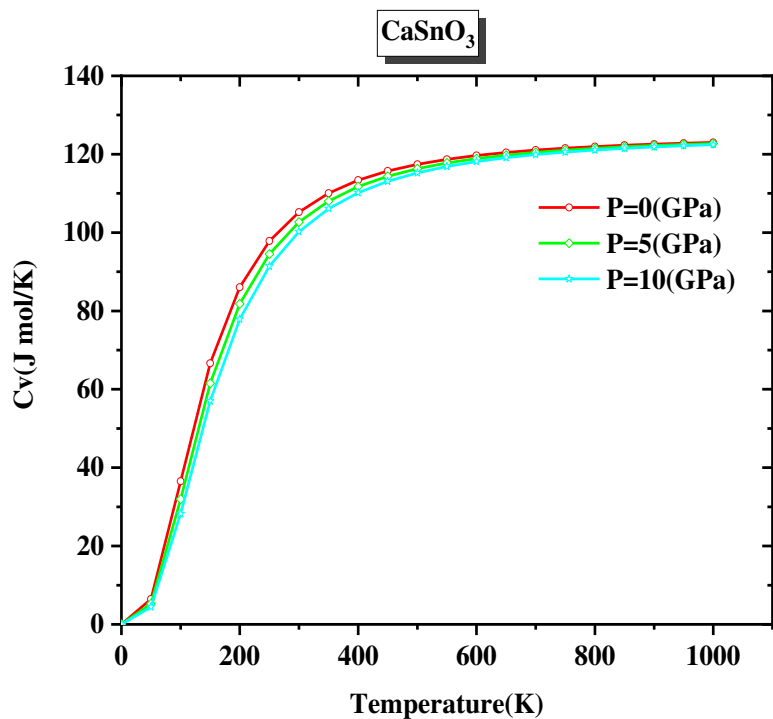


FIGURE II-8: variation of the heat capacity " $C_v$ " of the compound  $CaSnO_3$  as a function of temperature.

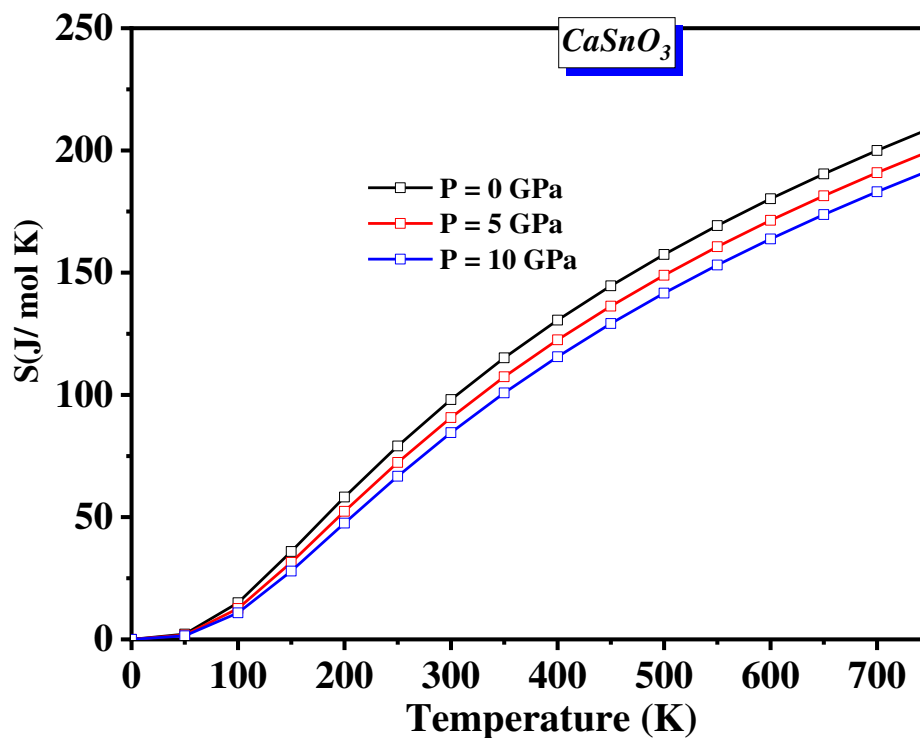
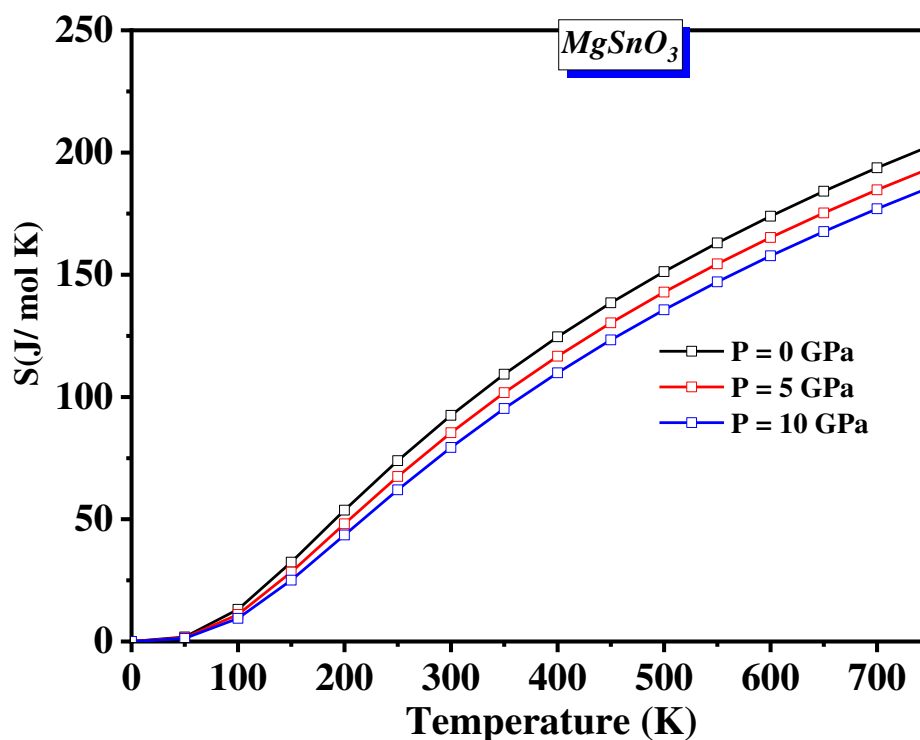
## 2-4 Entropy

Thermodynamic entropy can be defined at two levels: on the microscopic level, entropy represents a measure of system disorder (chaos and randomness) or the number of possible states that any system can take. This is expressed as  $S = k \ln \Omega$  (II.4)

where  $\Omega$  represents the number of possibilities or arrangements that a compound can occupy, while  $k$  represents the Boltzmann constant. On the macroscopic level, entropy is the amount of internal energy of a substance that cannot be converted into useful work and can be considered as unusable energy for obtaining work [25,26].

The value of entropy for a substance is related to its internal compositions and is influenced by several factors. When the entropy value increases, it leads to numerous changes in the internal structure of the compound, such as atomic vibrations deviating from their equilibrium positions, electrons transitioning from one electronic level to another, or changes in the random occupation of atomic sites in the crystalline lattice [25,26].

During our study of changes in entropy under the influence of two important factors in nature, namely temperature and pressure, we observed from the diagrams shown in Figure (II.9) that the entropy of the  $\text{MgSnO}_3$  and  $\text{CaSnO}_3$  compounds have the same behavior and influenced by temperature effect, where we can see a proportional relationship between entropy changes and temperature. This is justified by the fact that the  $\text{MgSnO}_3$  compound, under the influence of temperature has new configurations.

FIGURE II-9: Variation of entropy (S) as function of temperature for  $\text{CaSnO}_3$ .FIGURE II-10: variation of the entropy (S) as function of temperature of  $\text{MgSnO}_3$ .

### **4-3 Thermal Expansion Coefficient:**

The thermal behavior of solid materials used in electronic devices has considerable importance, especially for devices that emit significant heat to the external environment. Among the most important thermal properties of solid materials is the thermal expansion coefficient. This is because thermal expansion of the material can lead to breaking and damaging parts or other materials within the devices, or at least cause pressure that may affect their electronic properties [25,26]

Thermal expansion occurs as a result of the action of thermal energy on the material's atoms through rising their vibrations ( move away from their equilibrium position and from each other) . The thermal expansion coefficient is related to several factors, including the nature of the bonds between atoms as well as the packing factor in the material.[25,26]

The thermal expansion coefficient of the MgSnO<sub>3</sub> and CaSnO<sub>3</sub> compounds, calculated using the GIBBS2 program in a heating range up to 800 Kelvin and under the influence of an external pressure of up to 15 GPa, is depicted in curves shown in Figure (II.11). The obtained results indicate that the studied compound has a very rapid expansion capability at low temperatures (below 200 Kelvin), and the expansion coefficient increases at a slower rate at high temperatures.

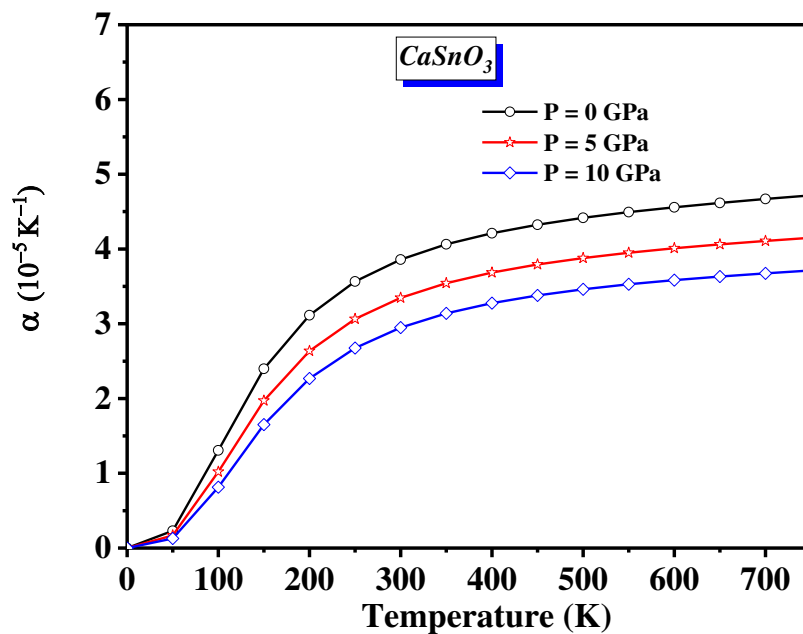


FIGURE II-11: variation of the thermal expansion coefficient ( $\alpha$ ) as function of temperature of  $\text{CaSnO}_3$ .

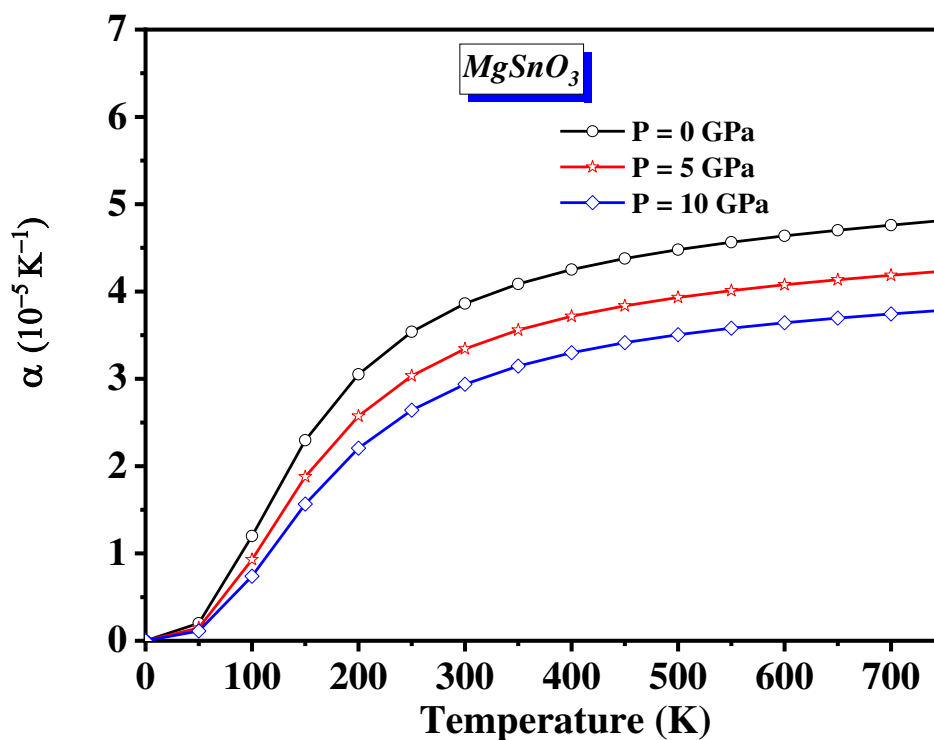


FIGURE II-12: variation of the thermal expansion coefficient ( $\alpha$ ) vary with changes in temperature of  $\text{MgSnO}_3$ .

## 5- Thermoelectric Properties

After examining the impact of heat on the thermal properties of solid materials, we will now explore the effect of temperature variation on the electrons within these materials. According to the article "Thermoelectric Devices: Principle and Future Trends"[28], materials exhibiting semiconductor behavior possess excellent thermoelectric properties. These materials are highly suitable for practical applications such as thermoelectric generators, thermal sensors, and thermoelectric motors. Given that  $\text{MgSnO}_3$  and  $\text{CaSnO}_3$  exhibit semiconductor behavior, we decided to investigate their thermoelectric properties, including the Seebeck coefficient, thermal conductivity, electrical conductivity, electronic specific heat capacity, and the ZT factor[26].

### 5-1 Seebeck Coefficient

The Seebeck coefficient, as an intrinsic electrical quantity, characterizes the solid material by describing the difference in electrical potential (voltage) between the ends of a material subjected to different temperatures.

Figure (II.13) and Figure (II.14) illustrates the changes in Seebeck coefficient with temperature for the  $\text{MgSnO}_3$  and  $\text{CaSnO}_3$  compounds. Through this figure, we noted the following points:

1. The values of the Seebeck coefficient are high at intermediate temperatures, between 300 and 400 Kelvin, while they are low at temperatures above 400 Kelvin.
2. The maximum value of the Seebeck coefficient recorded for temperatures confined within the range of 300-400 Kelvin is greater than 2.5 mV/K for  $\text{CaSnO}_3$  and 1.5 mV/K for  $\text{MgSnO}_3$ .

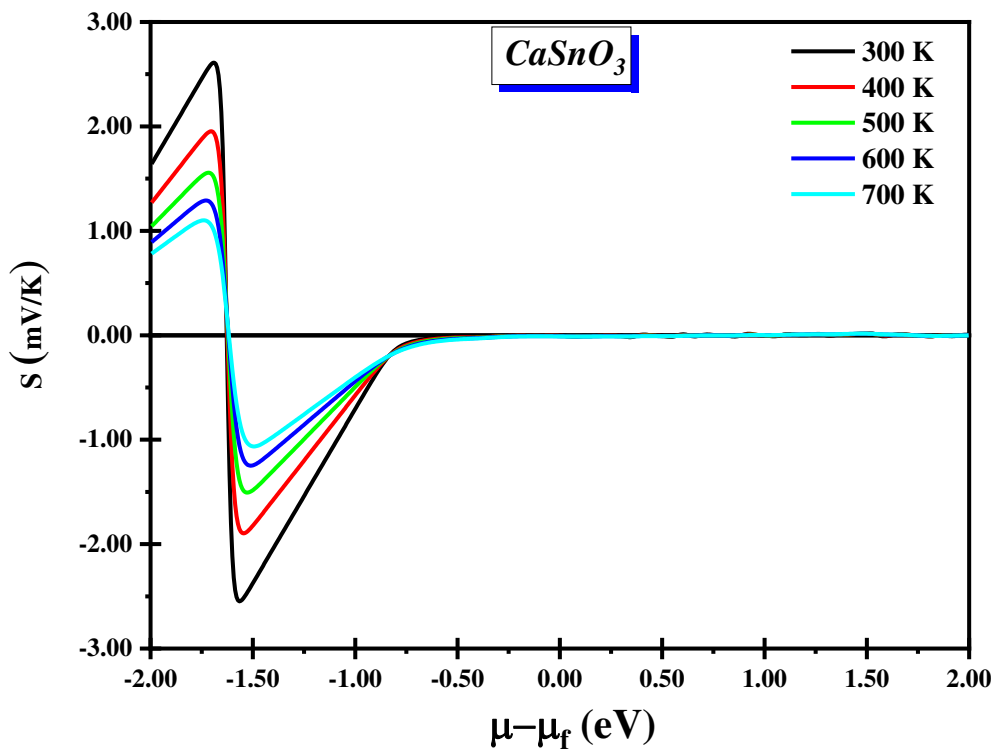


FIGURE II-13: Changes in the Seebeck coefficient at different temperatures vary with changes in chemical potential of  $\text{CaSnO}_3$ .

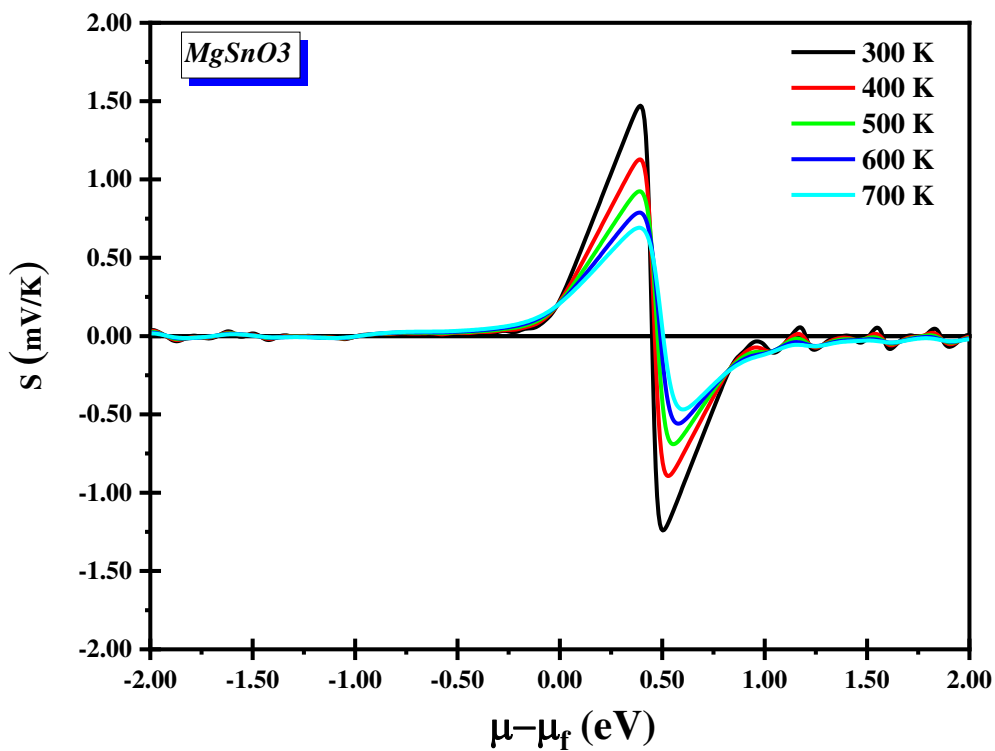


FIGURE II-14: Changes in the Seebeck coefficient at different temperatures vary with changes in chemical potential of  $\text{MgSnO}_3$ .

## 5- 2 Electrical Conductivity

Electrical conductivity (also known as electrical transport) of materials is another important characteristic in solid materials, as it represents the material's ability to conduct and carry electrical current. Electrical conductivity is linked to the internal structure of materials, their electronic behavior, and some external factors such as temperature, which leads to atomic vibrations and consequently to interactions between electrons (charge carriers) and phonons[26,29].

Figures (II.15) and (II.16) depicts the changes in electrical conductivity with temperature for the studied compound. Through this figures, we noted the following points:

1. Electrical conductivity is maximized within the chemical potential range [+0.5 ; 1 eV] for CaSnO<sub>3</sub> and [-1; -0.5 eV ]for MgSnO<sub>3</sub>.
2. As the temperature increases, the value of electrical conductivity decreases due to the increase in resistance caused by the more vibrations of the atoms in the crystalline lattice.

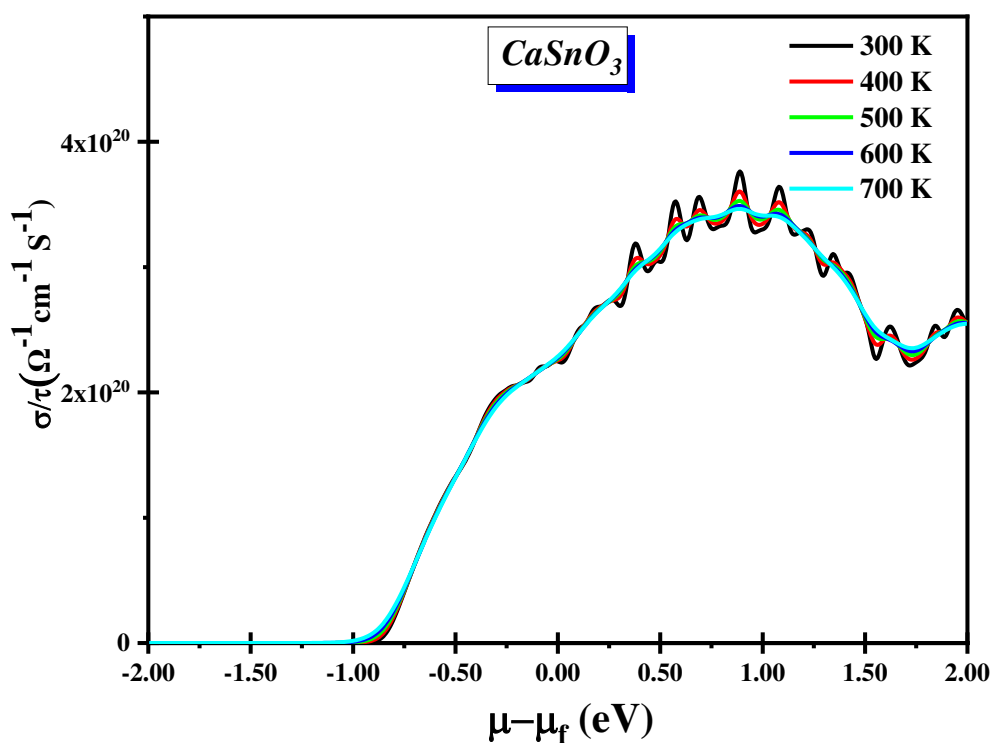


**FIGURE II-15:** The electrical conductivity at different temperatures varies with changes in the chemical potential for CaSnO<sub>3</sub> compound.

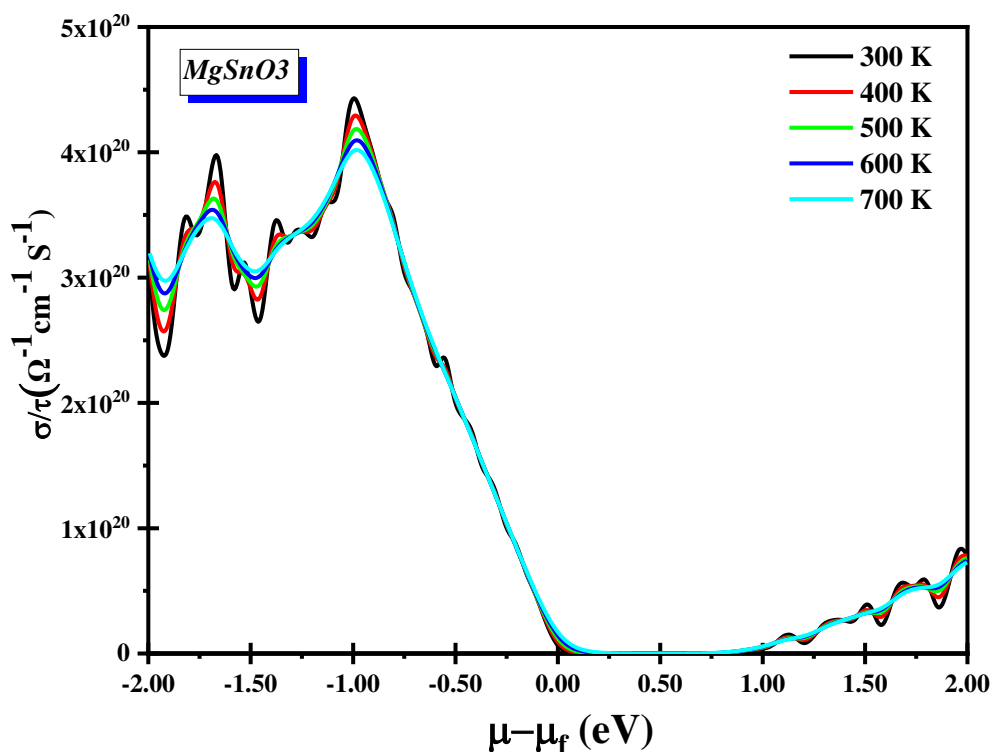


**FIGURE II-16:** The electrical conductivity at different temperatures varies with changes in chemical potential of MgSnO<sub>3</sub>.

### 5-3 Electronic Thermal Conductivity:

Charge carriers can also contribute to electrical conductivity, and there is a portion of heat transferred with the charge carriers[26,29].

Figure (II.17) illustrates the changes in electronic thermal conductivity with temperature for the studied compounds. Through this figure, we noted the following points:

1. The electronic thermal conductivity increases with temperature.
2. The thermal conductivity exhibits a similar behavior to electrical conductivity for both compounds. This relationship between electrical and thermal conductivities follows the Wiedemann-Franz law, given by:

$$K_e = L \sigma T \quad (\text{where } L \text{ is Lorentez number}) \quad (II.5)$$

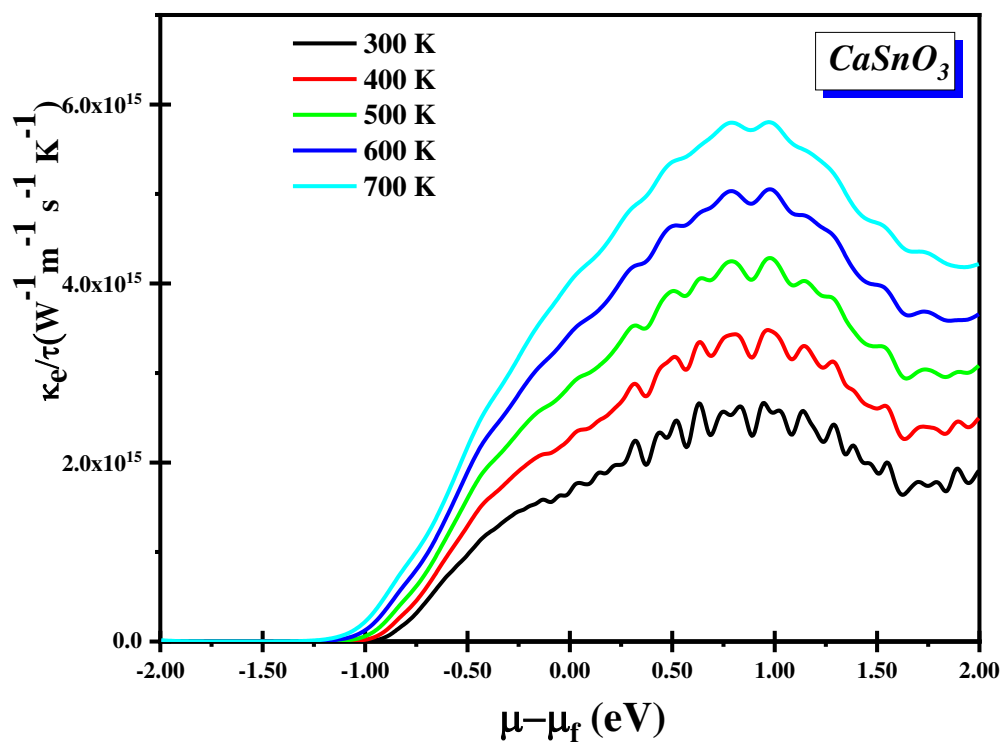


**FIGURE II-17:** The electronic thermal conductivity at different temperatures varies with changes in chemical potential of  $\text{CaSnO}_3$ .

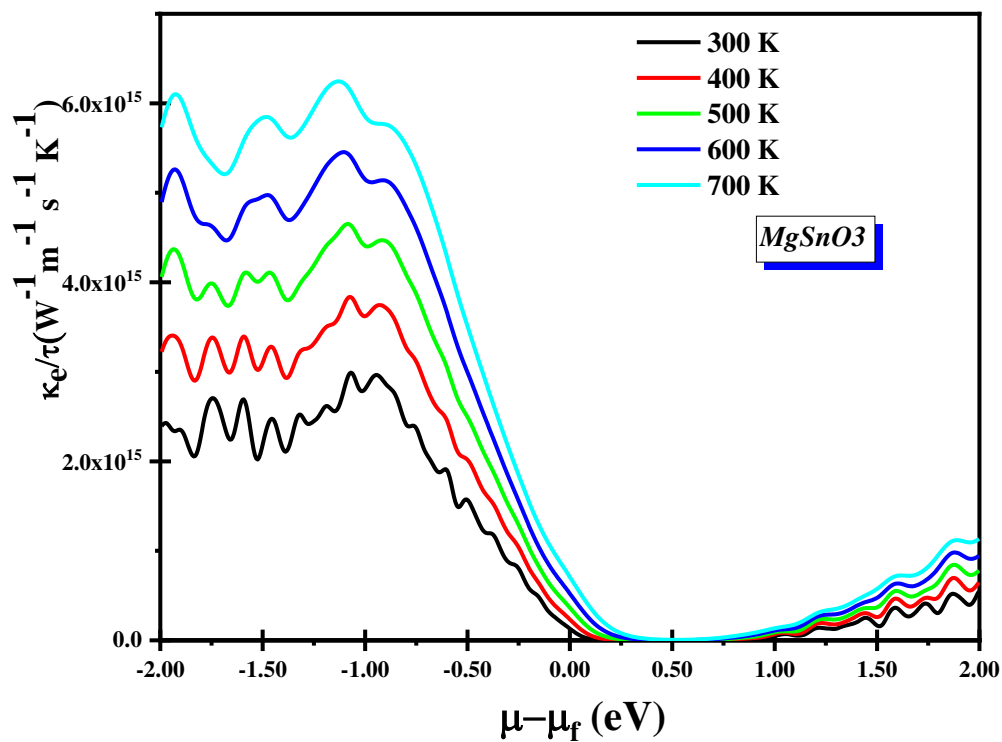


**FIGURE II-18:** The electronic thermal conductivity at different temperatures varies with changes in chemical potential of  $\text{MgSnO}_3$ .

### 5-4 ZT Factor

the optimal selection of materials for their thermoelectric efficiency is a key focus of both theoretical and experimental research. Evaluating the performance of thermoelectric materials involves assessing their figure of merit,  $ZT$ . The  $ZT$  value is a crucial parameter that quantifies the efficiency of a thermoelectric material, and it is determined using the following expression:

$$ZT = \frac{S^2 T \sigma}{\kappa} \quad (II.6)$$

Where:

- $S$  is the Seebeck coefficient,
- $\sigma$  is the electrical conductivity,
- $\kappa$  is the total thermal conductivity, and
- $T$  is the absolute temperature.

Figure (II.19) illustrates the variation of the figure of merit  $ZT$  at different temperatures with respect to changes in the chemical potential. Through this figures, we observe that the values of  $ZT$  for both compounds reached its maximum value ( $ZT=1$ ) when the chemical potential is confined in the range from [-1.5 to -0.5 eV] for all temperatures for  $\text{CaSnO}_3$  and between [-0.25 to 0.5 eV] for  $\text{MgSnO}_3$ .

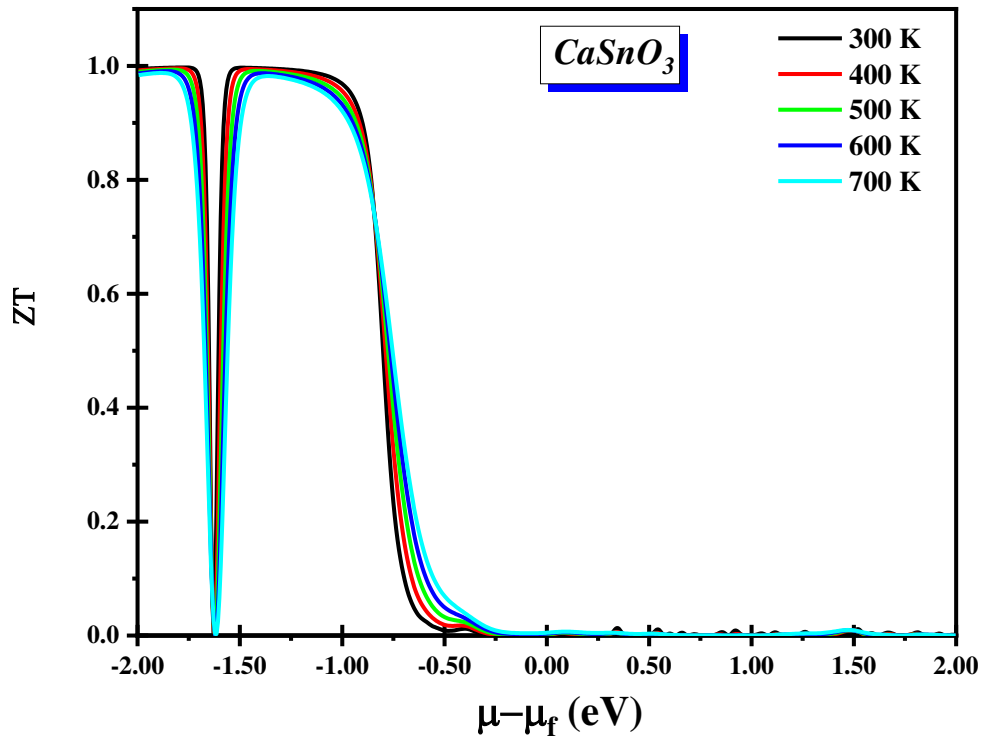


**FIGURE II-19:** The electrical conductivity at different temperatures varies with changes in chemical potential of  $\text{CaSnO}_3$ .

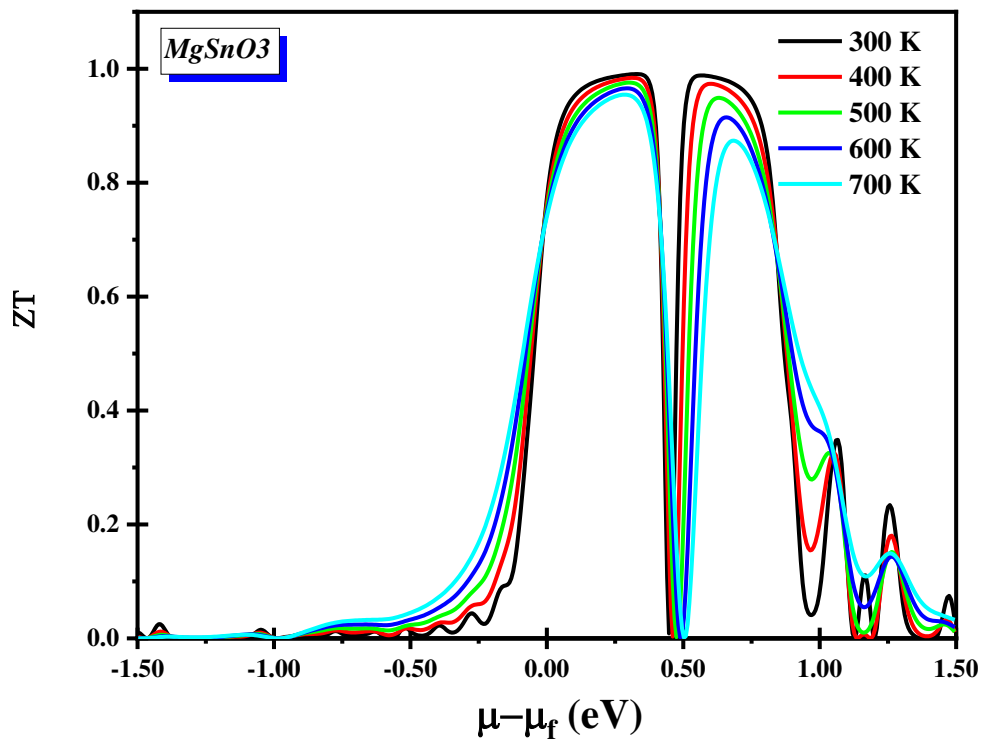


**FIGURE II-20:** The electrical conductivity at different temperatures varies with changes in chemical potential of  $\text{MgSnO}_3$ .

## 6) References

- [1] J C Slater *Phys. Rev.* **51** 840 (1937).
- [2] D D Koelling and G O Arbman *J. Phys. F Met. Phys.* **5** 2041 (1975).
- [3] O K Andersen *Phys. Rev. B* **12** 3060 (1975).
- [4] D R Hamann *Phys. Rev. Lett.* **42** 662 (1979).
- [5] D Singh and H Krakauer *Phys. Rev. B* **43** 1441 (1991).
- [6] E Sjöstedt, L Nordström, and D J Singh *Solid State Commun.* **114** 15 (2000).
- [7] P. Blaha, K. Schwarz, G. Madsen, D. Kvasnicka, J. Luitz (2001).
- [8] A Görling *Phys. Rev. A* **59** 3359 (1999).
- [9] P Hohenberg and W Kohn *Phys. Rev.* **136** B864 (1964).
- [10] Á Nagy *Phys. Rep.* **298** 1 (1998).
- [11] B T Sutcliffe *Fundam. Electron Density Density Matrix Density Funct. Theory At. Mol. Solid State* 3 (2003).
- [12] R G Parr *Horiz. Quantum Chem.* 5 (1980).
- [13] T A Wesolowski *Chall. Adv. Comput. Chem. Phys.* 153 n.d.
- [14] J P Perdew, K Burke, and M Ernzerhof *Phys. Rev. Lett.* **77** 3865 (1996).
- [15] G K Madsen and D J Singh *Comput. Phys. Commun.* **175** 67 (2006).
- [16] V L A. Otero-de-la-Roza, D. Abbasi-Pérez *Comput. Phys. Commun.* **182(10)** 2232 (2011).
- [17] V L A. Otero-de-la-Roza *Comput. Phys. Commun.* **182(8)** 1708 (2011).
- [18] O K Andersen and T Saha-Dasgupta *Phys. Rev. B* **62** R16219 (2000).
- [19] F Izumi and K Momma *Three-dimensional visualization in powder diffraction* (Trans Tech Publ) p 15 (2007).
- [20] K Momma and F Izumi *J. Appl. Crystallogr.* **44** 1272 (2011).
- [21] K Momma and F Izumi *J. Appl. Crystallogr.* **41** 653 (2008).
- [22] K Momma and F Izumi *Comm. Crystallogr Comput IUCr Newslett* **7** 106 (2006).
- [23] F D Murnaghan *Proc. Natl. Acad. Sci. U. S. A.* **30** 244 (1944).
- [24] A H Shakeel, S Khan, A Laref, G Murtaza, and J Bila *Opt. Mater.* **109** 110325 (2020).
- [25] S Saad Essaoud *DOCTORAT THESIS* (2020).
- [26] S S Essaoud and A S Jbara *J. Magn. Mater.* 167984 (2021).
- [27] A T Petit and P L Dulong *Ann Chim Phys* **10** 395 (1819).

- [28] I M Abdel-Motaleb and S M Qadri *ArXiv170407742 Cond-Mat* (2017).  
[29] Dilmi *PhD Thesis* (Université de M'sila) (2020).

## **CONCLUSION**

---

### Conclusion

In this study, we employed a program called Wien2k, which is primarily based on Density Functional Theory (DFT) for simulation purposes. DFT involves various approximations to handle the complex calculations of electronic structure, with the Generalized Gradient Approximation (GGA) being the specific method chosen for this research. The findings from this study can be summarized as follows:

- ✓ The compound  $\text{MgSnO}_3$  has a larger bulk modulus compared to the compound  $\text{CaSnO}_3$ , indicating that  $\text{MgSnO}_3$  is more resistant to pressure and less compressible.
- ✓ The energy gap for the  $\text{CaSnO}_3$  compound is found to be 1.13 eV (indirect band-gap  $\Gamma$ -M) using GGA approximations.
- ✓ The energy gap for the  $\text{MgSnO}_3$  compound is determined to be 0.76 eV (indirect band-gap  $\Gamma$ -M) using GGA approximations.
- ✓ For both compounds, the heat capacity  $C_v$  decreases linearly with increasing pressure, indicating a predictable response to pressure changes.
- ✓ The heat capacity  $C_v$  increases rapidly with rising temperature at low temperatures (below 200 Kelvin), and then approaches a limiting value at high temperatures, showing typical thermodynamic behavior.
- ✓ The Seebeck coefficient values are notably high at intermediate temperatures, specifically between 300 and 400 Kelvin.
- ✓ The maximum value of the Seebeck coefficient recorded for temperatures confined within the range of 300-400 Kelvin is greater than 2.5 mV/K for  $\text{CaSnO}_3$  and 1.5 mV/K for  $\text{MgSnO}_3$ .
- ✓ Electrical conductivity is maximized within the chemical potential range of [+0.5 to 1.0 eV] for  $\text{CaSnO}_3$  and [-1.0 to -0.5 eV] for  $\text{MgSnO}_3$ , suggesting optimal doping levels for electrical performance.
- ✓ For both compounds, as the temperature increases, the values of electrical and thermal conductivities also increase. This parallel behavior suggests that both properties are closely related in these materials.

## ملخص

في عملنا هذا أجرينا دراسة نظرية لحساب الخواص البنيوية ، الإلكترونية ، الترموديناميكية والكهروحرارية للمركبين  $\text{CaSnO}_3$  و  $\text{MgSnO}_3$  باستخدام طريقة الأمواج المستوية المتزايدة خطياً (FP-LAPW) المعتمدة على نظرية دالية الكثافة (DFT). لحساب الكمون تبادل-ارتباط استعملنا تقريب التدرج المعمم  $GGA$  في دراسة خواص المركبين. في حساب الخواص البنيوية، قمنا بحساب ثابت الشبكة، معامل الانضغاطية ولفهم السلوك الإلكتروني لكلا المركبين قمنا بتحليل بنية عصابات الطاقة الإلكترونية وأطياف الكثافة الحالات الإلكترونية DOS الكلية والجزئية. في حساب الخواص الترموديناميكية، ركزنا على حساب بعض المقادير الحرارية معينة باستخدام نموذج ديبياي الشبه التوافقي ، حيث سمح لنا بدراسة تأثير درجة الحرارة والضغط على بعض المقادير مثل السعات الحرارية  $C_v$  ، معامل التمدد الحراري  $\alpha$  ، الأنتروبييا. في نهاية قمنا بحساب الخواص الكهروحرارية كمعامل سيبك والناقلية الكهربائية والناقلية الحرارية الإلكترونية.

## Abstract

In our work, we conducted a theoretical study to calculate the structural, electronic, thermodynamic, and thermoelectric properties of the compounds  $\text{MgSnO}_3$  and  $\text{CaSnO}_3$  using the full-potential linearized augmented plane wave (FP-LAPW) method based on density functional theory (DFT). To calculate the exchange-correlation potential, we used the generalized gradient approximation (GGA) to study the properties of the compounds. In calculating the structural properties, we determined the lattice constant and the bulk modulus. To understand the electronic behavior of both compounds, we analyzed the electronic band structure and the density of states (DOS), both total and partial. In calculating the thermodynamic properties, we focused on determining certain thermal quantities using the quasi-harmonic Debye model, which allowed us to study the effect of temperature and pressure on quantities such as heat capacities  $C_v$ , thermal expansion coefficient  $\alpha$ , and entropy. Finally, we calculated the thermoelectric properties such as the Seebeck coefficient, electronic electrical conductivity, and electronic thermal conductivity.